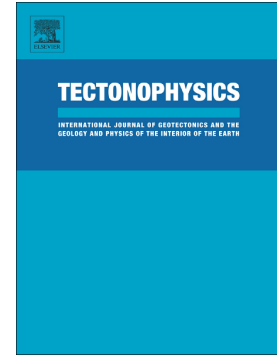


Accepted Manuscript

Tectonic interaction between Mesozoic to Cenozoic extensional and contractional structures in the Preandean Depression (23°–25°S): Geologic implications for the Central Andes

F. Martínez, C. López, S. Bascuñan, C. Arriagada

PII: S0040-1951(18)30259-2
DOI: doi:[10.1016/j.tecto.2018.07.016](https://doi.org/10.1016/j.tecto.2018.07.016)
Reference: TECTO 127892
To appear in: *Tectonophysics*
Received date: 5 March 2018
Revised date: 20 June 2018
Accepted date: 24 July 2018



Please cite this article as: F. Martínez, C. López, S. Bascuñan, C. Arriagada , Tectonic interaction between Mesozoic to Cenozoic extensional and contractional structures in the Preandean Depression (23°–25°S): Geologic implications for the Central Andes. Tecto (2018), doi:[10.1016/j.tecto.2018.07.016](https://doi.org/10.1016/j.tecto.2018.07.016)

This is a PDF file of an unedited manuscript that has been accepted for publication. As a service to our customers we are providing this early version of the manuscript. The manuscript will undergo copyediting, typesetting, and review of the resulting proof before it is published in its final form. Please note that during the production process errors may be discovered which could affect the content, and all legal disclaimers that apply to the journal pertain.

Tectonic interaction between Mesozoic to Cenozoic extensional and contractional structures in the Preandean Depression (23°-25°S): geologic implications for the Central Andes

Martínez, F^{*1}., López, C¹., Bascuñan, S²., Arriagada, C².

1. Departamento de Ciencias Geológicas, Universidad Católica del Norte, Angamos 0610, Antofagasta, Chile.
2. Departamento de Geología, FCFM, Universidad de Chile, Santiago, Chile.

*Corresponding author. Email: Fernando.martinez@ucn.cl; Tel: +569-85570079.

Abstract: A multidisciplinary study supported by field data and 2-D seismic information was conducted to understand the tectonic interactions between Mesozoic to Cenozoic extensional and contractional structures along the Preandean Depression (23°-25°S) in northern Chile, which have been largely debated. This work gives some new ideas about the control that ancient basement extensional faults exert on the crustal shortening and growth of those orogenic belts located over normal subduction zones similar to the Central Andes. In this work, two sedimentary basins were analyzed: the Salar de Atacama and the Salar de Punta Negra, both of which correspond to intra-montane basins bounded by the Domeyko Cordillera and the current volcanic arc of the Central Andes. The interpretation of a series of west to east-oriented 2-D seismic profiles revealed three types of structural interaction: i) pure positive reactivation; ii) decapitation of previous normal faults by reverse faults; and iii) transport of previous normal faults by thrust ramps. Inversion anticlines and basement-involved contractional structures were the most common observed structures, indicating that the geometry and distribution of inherited normal faults of the Paleozoic and Mesozoic basement played an important role in basin contraction. The different modes of tectonic interaction frequently created variations on the geometry and kinematic of the final structural styles present in the region. Commonly the Upper Cretaceous to Cenozoic synorogenic tectonosequences recorded the ages of contractional deformation that affected the region. Similar to other regions of northern Chile, basin inversion occurred during the Late Cretaceous and subsequent propagation of reverse faults occurred from the upper Late Cretaceous to the present. The basement-involved reverse fault structures usually create the most important positive topographic relief in this part of the western Central Andes. Using as example our study area, we finally conclude that the original position and distribution of ancient basement pre-orogenic normal faults in

the orogenic belts condition the final vergence and kinematic of the subsequent thrust systems related to shortening episodes.

Keywords: sedimentary basin; seismic profile; contraction; faults; tectonic interaction.

ACCEPTED MANUSCRIPT

1. Introduction

The Preandean Depression in northern Chile (Fig. 1) is one of five tectonic provinces of the forearc of the Central Andes. This province is located between the Domeyko Cordillera (or Chilean Precordillera) and the magmatic arc, and exhibits a significant negative structural relief, evidenced by a series of Cretaceous and Cenozoic NNE-oriented intra-montane basins (Figs. 1 and 2). Along the northern and central part of the depression, the Salar de Atacama and Punta Negra (Figs. 1 and 2) are the main basins, with an approximate area of 21,000 km². Both consist of topographic lows occupied by salt flats and mostly sedimentary (Cretaceous)-Tertiary continental deposits. Here, the salt flats and more recent continental deposits mostly prevent observation of their internal structure and complete stratigraphic record.

Regional studies (e.g., Arriagada et al., 2006; Jordan et al., 2002; 2007; Martínez et al., 2017; Muñoz et al., 2002; Pananont et al., 2004) have taken advantage of 2-D seismic information to interpret the structure and deformation history of the Preandean Depression and most major efforts have involved the northern part along the Salar de Atacama Basin as it contains a complete set of geological information that includes oil well data, gravity and seismic profiles (Fig. 3), and some field data from its western section. These studies have attempted to explain the structure of the region using different tectonic models, which include: a) the Late Cretaceous tectonic inversion of a former Jurassic extensional basin (e.g., Tarapacá Basin; Arriagada et al., 2006; Bascuñan et al., 2016; Mpodozis et al., 2000; 2005; Muñoz, et al., 2002; Mpodozis and Ramos, 2008) that extended from northern Perú to northern Chile during Jurassic-Early Cretaceous; b) the creation of a flexural foreland basin during the Late Cretaceous (Flint et al., 1993; Hartley et al., 1992); c) the Cenozoic tectonic collapse of a pre-existing Eocene thrust system, and even Pliocene margin-parallel strike-slip deformation (Kuhn, 2002). More recent works (Martínez et al., 2017) in the Salar de Punta Negra Basin (Fig. 2) have interpreted the structure as the result of different superimposed extensional and contractional episodes active during the Mesozoic (extension) and Cenozoic (contraction).

The existence of different models indicates that the structure of the Preandean Depression is complex and not completely understood. Some works (Muñoz et al., 2002; Mpodozis et al., 2005; Martínez et al., 2017) agree that extensional and contractional structures played an important role during its evolution. Interactions between such structures are commonly observed in many basins of the Central Andes in Chile and Argentina (e.g., Salta Rift,

Santa Barbara System, Chañarcillo, and Neuquén basins; Carrera et al., 2006; Giambiagi et al., 2003; Kley, 1999; Martínez et al., 2013; Mescua and Giambiagi, 2012) and are frequently associated with the positive and/or negative reactivation of pre-existing basement structures. Although the surface geology of the Preandean Depression has been relatively well studied, the nature of the tectonic interaction between extensional and contractional structures on the subsurface remains a topic of debate. For example, previous studies have proposed different geometries for structures as the Salar Fault and the Barros Arana Syncline in the Salar de Atacama Basin (Fig. 3), thus revealing opposite interpretations to regional structures (Arriagada et al., 2006; Flint et al., 1993; Jordan et al., 2007; Pananont et al., 2004; Rubilar et al., 2018).

To understand the tectonic interactions between the Mesozoic and Cenozoic extensional and contractional structures in the central part of the Preandean Depression and their tectonic implications for the geological evolution of the western Central Andes, we present a new seismic and structural interpretation of 2-D seismic profiles of the Salar de Atacama and Punta Negra basins. In this study, we document the structural styles that result from this interaction and model the geometry of first-order faults considering the deformation style of their hanging wall blocks. We also determine the structural and stratigraphic characteristics of the seismic sequences involved in deformation. We finally documented as the original position and distribution of ancient basement pre-orogenic normal faults in the orogenic belts condition the final vergence and kinematic of the subsequent thrust systems related to Cenozoic shortening episodes. The results obtained here, could be used to compare similar structural relationships observed in other orogenic belts worldwide.

2. Geological setting

The northern and central part of the Preandean Depression in northern Chile (Fig. 2) is formed by two NNE-oriented intra-montane basins: the Salar de Atacama and Salar de Punta Negra basins. They form an area of negative relief between the Domeyko Cordillera and the Western Cordillera and/or magmatic arc (Fig. 2) with elevations between ~3000 and 2300 m.a.s.l. (Gardeweg et al., 1994; Makshev et al., 1999; Soto et al., 2005; Arriagada et al., 2006; Reutter et al., 2006; Martínez et al., 2017).

2.1. Salar de Atacama Basin

The Salar de Atacama Basin is the most studied region of the Preandean Depression. The use of field, oil well, and seismic data has revealed the distribution of major volcanic and sedimentary stratigraphic units beneath the basin. The oldest rocks in this region are mainly exposed in the Cordón de Lila along the southern termination of the basin (Figs. 2 and 3) and defined as the Lila Complex (Niemeyer, 1984). These consist of Lower Paleozoic sedimentary and igneous rocks (sandstones with intercalated pillow lavas) and some stratified volcanic and sedimentary deposits of Upper Paleozoic to Triassic age (Niemeyer, 1984; 1997), which are interpreted as the products of a former volcanic arc and shallow marine deposits (Niemeyer, 1989).

On surface, the Mesozoic rocks are mainly represented by stratified Cretaceous successions exposed to the east of the El Bordo Escarpment and along the Barros Arana Syncline on the northwest flank of the basin (Fig. 3). They consist of a thick (almost 4000 m) continental volcanic and sedimentary succession composed of conglomerates, laminated sandstones, gypsum layers, mudstones, and andesites, which form part of the Purilactis Group (Digman, 1963; Hartley et al., 1992; Charrier and Reutter, 1994; Mpodozis et al., 2005; Bascuñan et al., 2015). This is composed of the Tonel, Purilactis, Barros Arana, and Cerro Totola formations (Fig. 5a) that are commonly associated with fluvial, alluvial, and lacustrine deposits (Digman, 1963; Bascuñan et al., 2015). Recent U-Pb ages of detrital zircons have reported maximum depositional ages of 149 Ma for the lower section of the Purilactis Group and 73-79 Ma for its upper section exposed in the Barros Arana Syncline (Bascuñan et al., 2015; Fig. 3). Other research has reported K-Ar ages between ~66-40 Ma for the upper section of this succession, as well as some related intrusions (Mpodozis et al., 2005; Fig. 3). The lower sections of this group (Tonel Formation; Arriagada et al., 2006) frequently exhibit contractional growth strata that provide clear evidence for synorogenic accumulation since at least 149 Ma (Figs. 6a, b).

Such as it has been recognized by Arriagada et al., (2006) (Fig. 2b in this work), along the westernmost part of the basin, the Purilactis Group is unconformably covered by almost 1900 m of folded Paleocene and Eocene sedimentary rocks (Fig. 3), predominantly composed of orange stratified sandstones and gypsum known as the Naranja Formation and volcanic (tuffs) and sedimentary (conglomerates) succession defined as Loma Amarilla Formation (Digman, 1963; Ramírez and Gardewed, 1982; Hammerschmict et al., 1992; Mpodozis, et al., 1999; Arriagada et al., 2006). Mpodozis et al. (2005) reported K-Ar and $^{40}\text{Ar-Ar}^{39}$ ages of 39.9 ± 3 Ma and 43.8 ± 0.5 Ma, respectively, indicating an Eocene age.

Although both formations have been well reported at the surface, they have not been clearly identified under the basin using Toconao-1 oil well data (Muñoz et al., 1997, 2002) so their subsurface interpretation remains highly speculative. Oligocene and Miocene deposits are mostly exposed along the Cordillera de la Sal (Fig. 3), and also along the northern and southeastern edges of the basin (Fig. 3), where they are affected by mesoscale folds and reverse faults (Figs. 5b,c). The Oligocene section consist of evaporites and siliciclastic rocks (sandstones, conglomerates, and shales) assigned to the Paciencia Group composed of the San Pedro (Figs. 5c) and Tambores formations (Brüggen, 1934; Ramírez and Gardeweg, 1982; Marinovic and Lahsen, 1984; Flint et al., 1993). Both formations are associated with lacustrine and alluvial deposits and have K-Ar ages of approximately 26 Ma (Mpodozis et al., 2000). The Miocene consist of ignimbrites and other more recent volcanic products that lie unconformably over the folded sedimentary rocks of the upper sections of the Purilactis Group (Fig. 5c).

2.2. Salar de Punta Negra Basin

The oldest rocks of this basin are mostly exposed along the eastern Domeyko Cordillera and the eastern flank of the basin along the Sierra de Almeida (Fig. 4). These correspond to thick (>2000 m) successions of Paleozoic (Devonian to Carboniferous) to Lower Triassic volcanic and sedimentary deposits known as Zorritas and La Tabla formations, which are intruded by some Permian (280–200 Ma) granitoids (Cecioni and Frutos, 1975; Isaacson et al., 1985; Niemeyer et al., 1997; Maksaev and Zentilli, 1999; González et al., 2015; Rubinstein et al., 2016). These have been interpreted as the products of an ancient magmatic arc active during the Paleozoic on the western margin of Gondwana (Breitkreuz and Zeil, 1994; Breitkreuz and Van Schmus, 1996).

The Paleozoic rocks are commonly covered by Lower Mesozoic successions composed of continental and marine Upper Triassic and Jurassic stratified rocks exposed along a narrow N-S deformed belt (Fig. 4) in the western edge of the basin and the easternmost part of the Domeyko Cordillera. The Upper Triassic successions consist of andesitic and siliciclastic rocks made of sandstones, shales assigned to Sierra de Varas Formation (González et al., 2015; Fig. 8). In the eastern Domeyko Cordillera, the Triassic deposits are unconformably covered by marine Jurassic successions (Fig. 4) composed of calcareous sandstones, mudstones, limestones, and black shales defined as the Profeta Formation (Chong, 1973; Ardill et al., 1998). Both Triassic and Jurassic deposits exhibit

important changes of thickness and contain intra-formational normal faults (Amilibia et al., 2008). These characteristics suggest that they are syn-rift sequences related to the stratigraphic infill of ancient extensional basins (e.g., the Tarapacá and Profeta basins; Mpodozis and Ramos, 1989; 2008; Mpodozis and Cornejo, 1997; Sheuber and Gonzalez, 1999; Mpodozis et al., 2005).

Along the central part of the basin to the west of the Pampa del Salado Upper Oligocene-Lower Miocene deposits are exposed (Fig. 4). These consist of almost 1000 m of stratified gravels, sandstones, conglomerates, ignimbrites, and volcanic ash defined as the Pampa de Mulas Formation (Chong, 1973; Gardeweg et al., 1993; Marinovic et al., 1995; Fig. 4). These are traditionally correlated with rocks of the Paciencia Group in the Salar de Atacama Basin. Previous research based on seismic visualization recognized contractional growth strata in the Pampa de Mulas Formation, indicating that this corresponds to a continental synorogenic sequence (Martínez et al., 2017). To the central, east and south part, Mio-Pliocene rocks represent the youngest infill of the basin (Fig. 4). They correspond to sedimentary (mainly sandstones and conglomerates) and other volcanic flows that are preferentially exposed in the Pampa San Eulogio (Fig. 4). Martínez et al. (2017) also used the seismic configuration of these successions to interpret them as synorogenic deposits.

3. Surface structure of the study area

The most prominent structures in the study area are exposed along the western edges of both basins (Figs. 3 and 4). In the Salar de Atacama Basin, the El Bordo Escarpment, the Barros Arana Syncline, and the Cordillera de la Sal (Fig. 3) thin-skinned folded belt represent first-order structures. El Bordo Escarpment is a NNE-striking topographic scarp 900 m high that separates the Domeyko Cordillera and the Salar de Atacama Basin (Arriagada et al., 2006). Along this scarp, Paleozoic and Triassic rocks overlie Cretaceous deposits of the Purilactis Group (Fig. 3), which are frequently folded and faulted.

To the northernmost part of the basin, the NNE-striking Barros Arana Syncline (Fig. 3) is an open syncline that includes the complete succession of the Purilactis Group, and which narrows toward the south (Fig. 3). Along its western limb, the middle section of the Purilactis Group is detached by an east-dipping thrust exposed along the Llano de Quimal (Fig. 3; Arriagada et al., 2006). Its eastern limb is bounded by the NNE-striking La Escalera Fault (Becerra et al., 2014), which consists of a west-dipping reverse fault along

which the Purilactis Group overlies Miocene ignimbrites (Fig. 3). Previous analyses of 2-D seismic profiles have interpreted this structure as a syncline that formed over a shallow east-verging ramp (Arriagada et al., 2006).

The Cordillera de la Sal is a NNE-striking thin-skinned folded belt located in the Salar de Atacama Basin between the Llano de la Paciencia and the salt flats (Figures 3 and 6c). It is composed of a series of narrow and asymmetrical anticlines and synclines that exhibit an en echelon array and that commonly involve Oligocene deposits of the Paciencia Group. They consist of west and east-verging folds with cores of evaporitic rocks, bounded by NNE-striking, west and east-dipping thrusts (Fig. 6c) (Paciencia, Los Vientos and San Pedro faults; Becerra et al., 2014; Rubilar et al., 2018), forming a pop-up structure (Fig. 3). This structural style has frequently been interpreted as a thin-skinned deformation pattern resulting from eastern propagation of the Domeyko Cordillera (Muñoz et al., 2002). Other subsidiary and mesoscale reverse faults have been observed along the northernmost part of the Cordillera de la Sal that mainly affect the Oligocene sedimentary deposits of the San Pedro Formation and Miocene ignimbrites (Figs. 5b, 7a).

In the Salar de Punta Negra Basin, the main structures (Figures 4) are commonly highly eroded and/or covered by Quaternary gravels that hinder observations. They are related to NE-SW and N-S-striking basement-involved reverse faults that separate basement ridges (e.g., Sierra de Varas; Fig. 4) from narrow belts of folded and faulted syn-rifted Mesozoic rocks (predominantly Triassic and Jurassic). Escondida-Punta Negra Fault (Fig. 4) represents the main structure in this sector and consists of a large and NNE-striking fault, which was recently interpreted as the western master fault of the Salar de Punta Negra Basin (Martínez et al., 2017). This is a high-angle fault that joins Paleozoic rocks with Jurassic rocks and Pliocene and recent deposits (Fig. 4). Moreover, the western edge of the Salar de Punta Negra Basin is frequently marked by escarpments associated with west-dipping basement-related reverse faults (Fig. 7b). Different interpretations have suggested that these structures could be kilometric (>10 km length) basement strike-slip faults associated with transpressive deformation during the Eocene (Maksaev, 1990; Mpodozis et al., 1993; Tomlinson and Blanco, 1997); however, more recent studies supported by balanced cross sections and seismic interpretation along the eastern Domeyko Cordillera and the western site of the Salar de Punta Negra Basin have indicated that it corresponds to a partially inverted Mesozoic normal fault of the former Tarapacá Basin established in the region during Jurassic (Amilibia et al., 2008; Martínez et

al., 2017). Along the eastern part of the Salar de Punta Negra Basin, a series of east-dipping, basement-related reverse faults have been recognized to west and south of the Sierra de Almeida . Seismic profiles located near to this area (Pampa El Salado) show as these faults affect the Paleozoic rocks and also Oligocene deposits and Miocene ignimbrites and even the Recent cover of the basin (Martínez et al., 2017).

4. Methodology

In order to understand the interaction between extensional and contractional structures in the central part of the Preandean Depression, we interpreted a series of W-E 2-D seismic profiles distributed along the Salar de Atacama and Punta Negra basins (Figures 3 and 4). We interpreted those seismic profiles located in the central and southern parts of both basins, because they contain good examples of the tectonic interaction between Mesozoic to Cenozoic extensional and contractional structures. Seismic data were integrated with geological information from previous studies based on mapping at 1:100.000 scale (Padilla, 1985; Gardeweg et al., 1993, 1994; Becerra et al., 2014; González et al., 2015) and other stratigraphic data derived from the Toconao-1 oil well in the central part of the Salar de Atacama Basin. The seismic data consist of a two-dimensional (2-D) seismic survey acquired and facilitated by ENAP-Sipetrol, which was previously used to identify possible oil and gas prospects under the Preandean Depression. Based on the appearance and continuity of the seismic reflectors, we classified the data as of moderate to good quality, and is better quality in the Salar de Atacama Basin.

The seismic profiles were first filtered and then migrated in time so that the vertical scale is in seconds (TWT). The velocity and density information of Toconao-1 required for time-depth conversion of the seismic data was not available for this study. Nevertheless, previous research has already performed this conversion, which is only applicable to the Salar de Atacama Basin (Pananont et al., 2004). In order to document the along-strike variation of structures, we perform seismic and structural interpretation of five seismic profiles: three in the Salar de Atacama Basin and two in the Salar de Punta Negra Basin (Figs. 3 and 4, lines IG024, IG08b, IG016b, 1F016 and 2F004). Before interpreting the seismic data, we made a seismic amplitude model using 2-D Move software (Midland Valley) to obtain a better contrast, in which reflectors with high amplitudes were highlighted. Then, we correlated the main seismic reflectors with geological units exposed along the seismic lines. This approach was mainly applied to the Salar de Punta Negra

Basin due to the lack of available oil well data. On the other hand, we used the seismic and well data calibration (Muñoz et al., 2002; Jordan et al., 2007) from Toconao-1 in the Salar de Atacama Basin (Fig. 3) to correlate the first order sequences present under this basin. Considering that this study has a structural approach, we used a grayscale in the seismic profiles because it enables easy identification of faults.

Interpretation of the seismic profiles and modeling of the faults and folds was performed using the StructureSolver software of Nunns and Rogan Company, which allowed rapid and precise forward modeling of the structures. The structures were interpreted according to the following criteria: a) recognition of reflector cut-off; b) recognition of truncated reflectors related to thrust faults and angular unconformities; c) lateral changes of amplitude to identify faults; and d) changes in reflector dip associated with folds and faults. Other criteria included determining the change of thickness of the stratigraphic sequences on each side of the faults in order to interpret structural styles and deposition history.

4.1. Limitations of this study

The main limitations of this work are associated with the quality of some seismic profiles, specifically those in the Salar de Punta Negra Basin (Fig. 4). These are typically of moderate quality in the first two seconds and highlight the stratified geological units very well, further, the deepest parts of the basin and some basement-involved structures are poorly constrained with this data. The absence of borehole information also hinders identification and correlation of geological units present on the subsurface, as well as the time-depth conversion of the seismic profiles. The seismic data in the Salar de Punta Negra Basin is only constrained by correlation with the crystalline basement and stratified rocks exposed along its western and eastern parts.

In the Salar de Atacama Basin, the seismic data does not have a good control on Lower Mesozoic successions and this is better constrained in the Salar de Punta Negra Basin. As 2-D seismic profiles were used in this study, it is difficult to spatially differentiate all the geological formations described in the geological setting; therefore, we only interpret seismic tectonosequences. Considering these limitations, we recommend that this data is used only to understand first-order structures present in the study area.

5. Seismic and stratigraphic tectonosequences

The interpretation of seismic tectonosequences is based on the identification of seismic

reflector patterns and angular unconformities from seismic reflector terminations (e.g., on-laps, erosional truncations, top-laps, etc.) and contrasts of seismic amplitude. We associated the acoustic basement with the crystalline basement rocks of the basins, which are mostly composed of Paleozoic granitic rocks (geological setting).

These typically exhibit seismic reflectors with chaotic patterns that are very difficult to interpret and correlate. The upper surface is marked by a continuous reflector of high amplitude that represents the regional unconformity between the basement and the stratigraphic cover (Fig. 8). The stratigraphic cover includes the follow tectonosequences.

Tectonosequence 1. (T1, Fig. 8) This is composed of low-amplitude and semi-continuous reflectors that usually onlap against the top of the basement. In the Salar de Atacama Basin, it consists of a uniform package of parallel seismic reflectors (Fig. 8), but in the Salar de Punta Negra Basin, it consists of an asymmetric stratigraphic wedge that thickens toward the master faults and shows a geometry similar to that reported by syn-rift sequences.

The seismic reflectors of this tectonosequence usually correlate with Upper Paleozoic volcanic and sedimentary successions (rhyolitic volcanic rocks, sandstones, and conglomerates) of La Tabla and/or Zorritas formations (Fig. 8). In the Salar de Atacama Basin, these could correlate with the igneous and sedimentary successions of the Lila Complex (Fig. 8). Although these have been previously considered as basement rocks (geological setting) of the basins, their dominant seismic expression (wedge shapes) observed in the Salar de Punta Negra Basin indicates that they were accumulated under extensional conditions.

Tectonosequence 2. (T2, Fig. 8). This is composed of a series of parallel and variable high and low- amplitude reflectors (Fig. 8) forming a wedge shape that fill some half-graben structures. Its basal section is marked by an angular unconformity defined by the onlap terminations of their basal reflectors against the top of tectonosequence 1 (Fig. 8) and/or the top of the basement. In the Salar de Atacama Basin, this was drilled by the Toconao-1 oil well (Muñoz et al 2002; Jordan et al., 2007) and consists of sedimentary (sandstones, shales, mudstones) and volcanic rocks (e.g., tuff, lavas) that have been correlated with synorogenic deposits of the Upper Cretaceous-Paleocene Purilactis Group (e.g., Mpodozis et al., 2005; Arriagada et al., 2006; Bascuñan et al., 2015). However; its seismic expression is not geometrically compatible with that reported by synorogenic sequences,

because these not shown important variations on thickness over contractional structures. On the contrary, this is mostly associated with a syn-rift sequence. Based on this criteria, we suggest that these rocks could be older than the Purilactis Group and are likely part of the syn-rift Mesozoic successions (e.g., Sierra de Varas, El Profeta formations) identified beneath the Salar de Punta Negra Basin (Fig. 8).

Tectonosequence 3. (T3, Fig. 8) This consists of a thick package of low and high amplitude seismic reflectors that unconformably overlie tectonosequence 2 (Fig. 8). The reflectors frequently show onlap terminations against the top of the underlying tectonosequence 2 (Fig. 8). This also reveals the characteristic change of thickness over contractional structures (inversion anticlines, synclines, thrust faults; Figs. 10, 11 and 12) indicating that its accumulation was controlled by the relief created during contractional deformation. An angular unconformity is commonly recognized in this tectonosequence, which could be interpreted as the limit between Upper Cretaceous and Paleocene deposits, but, this is only identified in the central part to the Salar de Atacama Basin. To the south, this unconformity is not clearly visible. Samples from the Toconao-1 oil well have revealed a volcanoclastic composition (volcanoclastic sandstones, conglomerates, claystones) to this tectonosequence, which has been correlated with the Upper Cretaceous-Paleocene Purilactis Group and part of the Naranja Formation (Muñoz et al., 2002; Arriagada et al., 2006; Fig. 8). Following its seismic expression and previous interpretations, we interpret this complete package of reflectors as an Upper Cretaceous-Paleocene synorogenic sequence.

Tectonosequence 4. (T4, Fig. 8) This consists of intercalated low and high-amplitude reflectors that unconformably overlie tectonosequence 3 (Fig. 8). Similar to tectonosequence 3, this also shows important variations of thickness over contractional folds, characterizing a synorogenic character (Figs. 10 and 11). The basal reflectors of the younger tectonosequence 5 typically truncate its upper section (Fig. 8). Data from the Toconao-1 borehole indicate that this is composed of conglomerates, sandstones, and claystones correlated with the Eocene successions previously dated by Mpodozis et al., (2005) described in the geological setting, even, fission-track ages of sandstone clasts have also indicated an Eocene age for this unit (Muñoz et al., 2002) . Following the interpreted stratigraphic record for the Salar de Atacama Basin (Muñoz et al., 2002; Arriagada et al., 2006) and the northern part of the Salar de Punta Negra Basin, we correlated this tectonosequence with Eocene sedimentary deposits (Loma Amarilla

Formation; Fig. 8).

Tectonosequence 5. (T5, Fig. 8) This predominantly consists of a series of continuous and parallel high-amplitude seismic reflectors (Fig. 8) that form an extensive cover mostly recognized along the central part of the Salar de Atacama Basin and central and southernmost parts of the Salar de Punta Negra Basin. The basal reflectors frequently onlap against the top of tectonosequence 4; however, these terminations are only observed in some sectors (Figs. 10 and 11). A strong reflector typically marks the top of this tectonosequence. Samples from the Toconao- 1 well and others taken from outcrops indicate that it consists of sedimentary rocks that include interstratified Oligocene-Miocene conglomerates, sandstones, gravels, ignimbrites, and other subordinate volcanic products that have been correlated with the Oligocene-Miocene Paciencia Group and/or Pampa de Mulas Formation (Fig. 8). These frequently thicken toward the frontal and back-limb of folded structures, thereby indicating a synorogenic character.

Tectonosequence 6. (T6, Fig. 8) This is a package of variable reflectors of high and low amplitude that overlie tectonosequence 6 (Fig. 8). The base is defined by an angular unconformity over which the basal reflectors commonly onlap against the limbs of contractional folds (Figs. 10 and 11). This is the youngest tectonosequence that infills both basins. Information from subsurface (Toconao-1 well) and surface indicate that this consists of volcanic and sedimentary rocks (sandstones, gravels, evaporites, and ignimbrites) correlated with Mio-Pliocene deposits, some of which show contractional growth strata, indicating a synorogenic nature.

6. Relationship between extensional and contractional structures

Based on our seismic and structural interpretation, interactions between extensional and contractional structures occur in three ways: a) pure positive reactivation of previous normal faults; b) decapitation of previous normal faults by reverse faults; and c) transport of previous normal faults over thrust ramps (Fig. 9).

6.1. Pure positive reactivation

Pure positive reactivation is represented by the tectonic inversion of inherent basement normal faults that form part of asymmetrical half-graben structures and opposite dipping normal faults separated by basement structural highs and/or horst blocks (Fig. 10).

Structures related to this tectonic process are usually observed in the central and southern end of the Salar de Atacama Basin (Figs. 10,11,12) and the north and central part of the Salar de Punta Negra Basin (Figs. 14 and 15). The seismic profiles located in both areas have highlighted large asymmetrical and doubly-verging anticlines with arrowhead shapes that involve Upper Paleozoic and Mesozoic stratigraphic wedges (tectonosequences TS1 and TS2; see details in seismic and stratigraphic tectonosequences). The stratigraphic wedges usually thicken toward the fault planes and the anticlines typically have long wavelengths with short, steep frontal limbs and large, sub-horizontal back limbs. This geometry is commonly acquired by the folding of syn-rift wedges when the slip of previous normal faults is reversed; therefore, this geometry evidences positive reactivation of previous normal faults (Figs. 10, 12, 14, 15). The anticlines frequently affect the hanging wall of ancient basement normal faults and their current tectonic vergence is strongly conditioned by the initial dip. Some buttress folds preserved under the Salar de Punta Negra Basin (Fig. 15) are narrow with overturned frontal limbs thus indicating that have been shortened and buttressed against the reactivated normal faults. Usually, the reactivated normal faults vary between faults with moderate angle, listric geometry and faults with high-angle, planar geometry. The majority of the normal faults have been partially reactivated; only some were fully reactivated and are mostly observed in the Salar de Punta Negra Basin (Figs. 14 and 15). Some inversion anticlines have been partially eroded and covered by synorogenic deposits related to the tectonosequences 3, 4 and/or 6. This situation is mostly associated with the areal distribution of the synorogenic deposits over the inverted structures. Recent research has interpreted similar partially inverted structures in the northern part of the Salar de Atacama Basin (Rubilar et al., 2017), indicating that structures exposed in this sector resulted from tectonic inversion of inherited basement normal faults.

6.2. Decapitation of previous normal faults by reverse faults

This type of structural interaction is mainly interpreted in the southern end of the Salar de Atacama Basin (Figs. 11, 12 and 13) and the northern region of the Salar de Punta Negra Basin (Fig. 14). It consists of basement-involved reverse faults that typically cut the upper section of ancient reactivated or non-normal faults (Figs. 11-14). In the Salar de Atacama Basin, the crystalline basement rocks of the Cordon de Lila are uplifted by east-dipping reverse faults (e.g., Salar Fault; Fig. 12); however, the seismic profiles transverse to these faults show preserved inversion anticlines and reactivated normal faults at their footwall

blocks, indicating that the reverse faults decapitated part of the upper section of previously reactivated normal faults (Figs. 11, 12). This situation is also observed to the east of the Cordon de Lila (Fig. 12), where characteristic changes of thickness in the syn-rift deposits related to the tectonosequence T2 are recognized in the hanging wall and footwall of the basement-involved reverse faults. Commonly these have greater thickness at the footwall block of the reverse faults, which is unusual considering that they were accumulated previous to the contractional deformation (Fig. 12). This structural and stratigraphic relationship indicates that some previous normal faults were decapitated by younger basement-involved reverse faults. Similarly, in the northern region of the Salar de Punta Negra Basin, an east-dipping basement-involved reverse fault placed the Paleozoic basement rocks over a stratigraphic wedge composed of syn-rift tectonosequences 1 and 2 (Fig. 14). The basement rocks form part of the footwall block of a previous normal fault, which is quite similar to those situation observed to the east of the Cordon de Lila; therefore, we interpret that the reverse fault decapitated the upper section of ancient normal faults, even, the seismic profiles of this region have highlighted part of this ancient normal fault (Fig. 14), which is characterized by a high amplitude seismic reflector. Previous research carried out in the Salar de Punta Negra Basin has suggested that some of the normal faults were positively inverted prior to their decapitation (Martínez et al., 2017). The last is confirmed considering the fact that some partially inverted faults in the southern end of the Salar de Atacama have been deformed and cut by basement-involved reverse faults (Figs. 11, 12 and 13). Commonly the upper section of the reverse faults has high angles, which are commonly confused with high angle normal faults (Pananont et al., 2004; Rubilar et al., 2017, among others). This structural relationship suggests that some of the original normal faults helped localize new basement-involved reverse faults. This process occurs when some inverted normal faults acquire a high angle and are locked during the basin contraction thus facilitating that they are cut.

6.3. Transport of previous normal faults by thrust ramps

This structural relationship has mainly been interpreted to the west of the Cordon de Lila in the Salar de Atacama Basin (Fig. 13). Seismic profiles in this region have highlighted a series of west-dipping high angle planar normal faults at the hanging wall block of a large east-dipping basement thrust ramp (Fig. 13), which is related to the westward continuity of the Salar Fault interpreted on the figure 12. The lower sections of normal faults are typically truncated along the lower section of the thrust ramp, indicating that they were

eastward passively transported through the basement thrust ramp. In contrast to other normal faults, these do not show evidence of positive reactivation and are generally buried by synorogenic deposits related to tectonosequences T3-T6. These faults correspond to antithetic normal faults that affect the hanging wall block of an ancient Mesozoic rollover structure, which is related to an east-dipping Mesozoic basement normal master fault. These antithetic normal faults controlled the accumulation of the syn-rift Mesozoic deposits associated with the tectonosequence T2 (Fig. 10). Although their lower sections usually are poorly highlighted by the seismic profile, we interpreted that they have been cut and them passively transported by the basement thrust ramp. The ramp corresponds to a low angle west-dipping high seismic amplitude reflector, which is partially highlighted by the seismic data (Fig. 11). We interpreted that this structure favored the uplift and exposure of the Paleozoic rocks along the Cordon de Lila (Fig. 3). The structure of the footwall of the thrust ramp has not sufficiently been highlighted by the seismic data and therefore is unknown. We suppose that the footwall block also is mainly composed of Paleozoic basement rocks.

Similar situations have been interpreted in other regions of the Central Andes, such as the Chilean Frontal Cordillera (Martínez et al., 2016), the Cuyo Basin in Argentina (Giambiagi et al., 2003) and the Eastern Cordillera of Peru (Pérez et al., 2016). Usually, this situation occurs when the initial dip angle of the previous normal faults is relatively high ($>45^\circ$), so that they cannot be reactivated and finally are cut and transported by new contractional structures. It is very possible that the new basement thrust ramp have taken advantage of the basal detachment of the previous normal faults, because this has an angle dip favorable to guide the contractional deformation, but, this is an only a hypothesis. Commonly, this structural style is associated with high degrees of crustal shortening. These thrust ramps are considered the most favorable structures to accommodate the Cenozoic crustal shortening interpreted in the region, since they allow to duplicate the original thickness of the upper continental crust and can cause greater subsidence.

7. Discussion

The results obtained from our new seismic and structural interpretations allowed us to document the role of ancient extensional and/or normal faults during progressive deformation of the study Andean region. Many large contractional structures buried beneath the Preandean basins used basement normal faults during their propagation thus

indicating that the interaction between normal and contractional structures was an important process during the shortening of this part of the Central Andes. The tectonic interaction between basement normal and reverse/thrust faults is a common process, which generally occurs in the first growth stages of orogenic belts (Sciciani et al., 2002), however; the previous normal faults also could be positively reactivated during different shortening episodes during the evolution of the orogens.

The oldest normal faults in the Preandean Depression are thought to result from earliest Late Paleozoic to Mesozoic extensional deformation episodes, as has been observed in neighboring regions in Chile (e.g., Domeyko Cordillera; Amilibia et al., 2008) and Argentina (e.g., Salta Rift; Kley et al., 2005; Carrera et al., 2006; Monaldi et al., 2008). Nevertheless, the existence of Mesozoic inherited basement normal faults along and under the Preandean basins has always been questioned, because there are few outcrops of Mesozoic (e.g., Jurassic and Lower Cretaceous) syn-rift deposits and on the contrary, most of the exposures of these deposits are restricted to the Domeyko Cordillera in Chile and other basins in Argentina. Nevertheless, some interpretations have suggested that contractional structures observed in regions as the Salar de Atacama could have originated from the tectonic inversion of ancient Mesozoic normal faults (Muñoz et al., 2002; Mpodozis et al., 2005) related to the Tarapacá back-arc extensional-related basin.

Some relevant evidence of this tectonic process, such as the occurrence of deformed syn-rift stratigraphic wedges, reactivated normal faults and inversion anticlines, among others, has not commonly been reported to the Preandean basins. Only a recent study in the Salar de Punta Negra demonstrated the existence of inverted Mesozoic half-graben structures under this basin (Martínez et al., 2017), thus supporting the previous structural interpretations of the Salar de Atacama Basin. In the current study, we have interpreted a series of Upper Paleozoic and Mesozoic stratigraphic wedges related to syn-rift deposits in the lower parts of the Preandean basins, which strongly evidence that this study region was tectonically extended prior to crustal shortening experienced during the Andean deformation, however; the magnitude and orientation of this crustal extension is still highly speculative.

In the region, positive reactivation of these normal faults is typically expressed by the presence of inversion anticlines on their hanging wall blocks. Although we have not restored these structures, we supposed that only those preferably oriented perpendicular

to the position of the regional contractional stress field and with low and moderate initial dip angles ($\leq 45^\circ$) were reactivated, such as has usually been documented by some experimental models (Bonini et al, 2012 and references herein). In both Salar de Atacama and Salar de Punta Negra basins, many of the inversion anticlines are unconformably covered by Upper Cretaceous synorogenic deposits, indicating that basin inversion was initiated during this time. Others inverted structures are directly covered by synorogenic Oligocene deposits, indicating that some normal faults were later reactivated (Martínez et al., 2017). Similar structural and stratigraphic relationships are interpreted in other basins in northern Chile (e.g., Chañarcillo, Lautaro basins), even in some parts of the Chilean Coastal Cordillera, indicating that initial contraction of Mesozoic back-arc related extensional basins in Chile was common during this time (Late Cretaceous), which is associated with the Peruvian tectonic phase (Jaillard, 1992).

Some inverted and/or normal faults are decapitated and/or transported by basement-related reverse faults and thrust ramps. The reverse faults typically affect the upper segments of the inverted and/or normal faults with opposite dip to these. These situations have been commonly interpreted in other regions of the Central Andes in Chile and Argentina, such as: the Lagunillas Basin (Martínez et al., 2016), Salta Rift (Carrera et al., 2006), El Metán Basin (Iaffá et al., 2011) and the Cuyo basins (Giambiagi et al., 2003), the Eastern Cordillera of Peru (Pérez et al., 2016) and also in other deformed belts around the world, such as the Apennines (Scisciani et al, 2002; 2009), the Alps (Butler et al, 1989; 2006), the Colombian Andes (Mora et al., 2009, 2010). Usually, this occurs when the initial dip angle of the previous normal faults is relatively high ($>45^\circ$), so that they cannot be reactivated and finally are cut and transported by new contractional structures. This interplay generally occurs from the steepening of reactivated normal faults, which result in locking and deformation by new reverse faults.

Considering the geometry of synorogenic tectonosequences T3-T6, we interpret that the basement-involved contractional structures are contemporaneous with accumulation of these sequences. Field data (tectonic escarpments) indicate that some may even exhibit recent activity. Previous studies have suggested that evolution of the Preandean Depression was interrupted by an important tectonic collapse during the Oligocene, causing the creation of normal faults (Jordan et al., 2007; Rubilar et al., 2017). We did not identify extensional structures and, in contrast, the tectonosequences associated with the Oligocene succession were mostly accumulated during the propagation of contractional

structures.

The interaction between extensional and contractional structures observed in the Preandean Depression is similar to those recognized in other regions of the Central Andes, especially in the Chilean Frontal Cordillera (Martínez et al., 2016). Although tectonic inversion played an important role during initial deformation of the region, the basement-involved reverse faults and thrusts resulted in the most important structures for crustal uplift, such as those identified in other neighboring regions (Domeyko Cordillera; Maksaev et al., 1999). Previous studies based on apatite fission track analyses have argued that these reverse faults propagated rapidly after the Eocene (Maksaev et al., 1999). Furthermore, the occurrence of angular unconformities between Cenozoic synorogenic deposits indicate that Andean deformation occurred diachronically in successive pulses (Paleocene, Eocene, Oligocene, Miocene, and even recent times). We suggest that the tectonic evolution of the Preandean basin occurred in three stages: i) Late Paleozoic-Mesozoic crustal extension and creation of half-graben structures; ii) Late Cretaceous tectonic inversion of half-graben structures; and iii) upper Late Cretaceous (?) and Cenozoic crustal shortening and creation of basement-involved reverse faults and thrust ramps.

8. Concluding remarks

A combination of field data and seismic profiles of two Preandean basins (Salar de Atacama and Salar de Punta Negra) was used to identify the presence and influence of pre-orogenic and ancient normal faults over the Andean contractional structures. Our results indicate that:

- Exits a serie of ancient normal faults under the Preandean Depression of the Central Andes, which have been clearly highlighted by the seismic data.
- The structure of this region consists of doubly-vergent inverted and basement-involved contractional structures, which suggest that important tectonic interactions between extensional and contractional structures occurred during its tectonic evolution. Usually, the original distribution of the normal faults, finally condition the final geometry and kinematics of the thrusts and reverse faults. The normal faults can be tectonically reactivated and/or decapitated depending of their initial geometry.

- The selective tectonic inversion of Late Paleozoic and Mesozoic half-graben structures previously established in this part of the Central Andes favored the creation of an initial relief composed of inversion anticlines, along which thick Upper Paleozoic and Mesozoic syn-rifted deposits were extruded and partially eroded.
- The seismic data show as the structural vergence of the contractional structures in the region is strongly conditioned by the initial dip of the ancient normal faults. It is a good example of how these are responsible for the along-strike variation of structural styles in orogenic belts established in regions that have been previously extended.
- Upper Cretaceous synorogenic deposits over the inversion anticlines commonly recorded the initial contraction of previous normal faults, while Cenozoic synorogenic deposits were mostly accumulated during propagation of large basement-involved reverse faults. This situation correlates very well with some interpretations made for many inverted basins in South America, which suggest that Paleozoic and Mesozoic half-graben structures were reactivated early during the Late Cretaceous.
- Successive Cenozoic crustal shortening of the region triggered propagation of east and west-vergent basement-involved reverse faults that partially modified the initial geometry of both inverted structures and/or normal faults. These structures appear to be responsible for the crustal uplift of the western and eastern edges of the basins, which represented the most important topographic relief in the region.

Acknowledgments

This work was supported by the Fondecyt project 11170098 "*Structure and tectonic evolution of the Pre-Andean Depression, Central Andes: case study of the Salar de Punta Negra Basin*". We acknowledge Dr. Lisandro Rojas and the ENAP-SIPETROL Company for providing the seismic data, and the Nunns and Rogan Company for providing the academic license of the StructureSolver software used for seismic and structural interpretation. Special thanks are given to Luis Acevedo for Landsat image support and Rodrigo Riquelme for constructive conversations. Finally, we thank the constructive comments and suggestions from two anonymous reviewers that benefited this work.

References

Amilibia, F. Sabat, K.R. McClay, J.A. Muñoz, E. Roca, G. Chong. 2008. The role of inherited tectono-sedimentary architecture in the development of the central Andean mountain belt: Insights from the Cordillera de Domeyko, vol. 30, pag., 1520–1539. *Journal of Structural Geology*.

Ardill, J., Flint, S., Chong, G., Wilke, H., 1998. Sequence stratigraphy of the Mesozoic Domeyko basin, northern Chile. *J. Geol. Soc. Lond.* 155, 71-88.

Arriagada, C., Cobbold, P.R., Roperch, P. 2006. The Salar de Atacama Basin: a record of Cretaceous to Paleogene compressional tectonics in the Central Andes. *Tectonics* 25: TC1008.

Bascuñán, S., Arriagada, C., Le Roux, J. and Deckart, K. 2016. Unraveling the Peruvian Phase of the Central Andes: stratigraphy, sedimentology and geochronology of the Salar de Atacama Basin (22°30–23°S), northern Chile. *Basin Res*, 28: 365–392. doi:10.1111/bre.12114.

Becerra, J., Henríquez, S.M., Arriagada, C., 2014. Geología del area Salar de Atacama, región de Antofagasta. Servicio Nacional de Geología y Minería. Carta Geológica de Chile, Serie Geología Básica 166: 111 p., 1 mapa escala 1:100.000. Santiago, Chile.

Bonini, M., Sani, F., Antonielli, B., 2012. Basin inversion and contractional reactivation of inherent normal faults: a review based on previous and new experimental models. *Tectonophysics* 522, 55–88.

Breitkreuz, C., Zeil, W., 1994. The late carboniferous to triassic volcanic belt in Northern Chile. In: Reutter, K.J., Scheuber, E., Wigger, P.J. (Eds.), *Tectonics of the Southern Andes*. Springer, pp. 277-292.

Breitkreuz, C., Van Schmus, W.R., 1996. U-Pb geochronology and significance of Late Permian ignimbrites timing of the magmatism of the paleo-pacific border of Gondwana: U-Pb geochronology in Northern Chile. *J. S. Am. Earth Sci.* 9, 281-293.

Brüggen, H. 1934. Grundzüge der Geologie und Lagerstättenkunde Chiles. Mathematische-Naturwissenschaftliche. Klasse, Heidelberger Akademie der Wissenschaften, Tübingen.

Butler, R.W.H., 1989. The influence of pre-existing basin structure on thrust system evolution in the Western Alps. In: Cooper, M.A., Williams, G.D. (Eds.), *Inversion Tectonics*. Geological Society of London, Special Publication, 44, pp. 105–122.

Butler, R.W.H., Tavarnelli, E., Grasso, M., 2006. Structural inheritance in mountain belts: an Alpine–Apennine perspective. *Journal of Structural Geology* 28, 1893-1908.

Carrera, N., Muñoz, J.A., Sabat, F., Roca, E., Mon, R., 2006. The role of inversion

tectonics in the structure of the Cordillera Oriental (NW Argentinean Andes). *J. Struct. Geol.* 28, 1921-1932.

Cecioni, A., Frutos, J., 1975. Primera noticia sobre el hallazgo de Paleozoico Inferior marino en la Sierra de Almeida, Norte de Chile. *Congr. Argent. Paleontol. Bioestratigr.* 1 (1), 191-207.

Charrier, R., Reutter, K. -J. 1994. The Purilactis Group of Northern Chile: Boundary between arc and backarc from late Cretaceous to Eocene In: REUTTER, K.-J., SCHEUBER, E. & WIGGER, P. (eds) *Tectonics of the Southern Central Andes*. Springer, Heidelberg, 189-202.

Chong, G., 1973. Reconocimiento geológico del área Catalina-Sierra de Varas y estratigrafía del Jurásico del Profeta, provincial de Antofagasta. Memoria de prueba. Departamento de Geología, Universidad de Chile, p. 284.

Dingman, R. J. 1963. Cuadrángulo Tolor, Provincia de Antofagasta. Instituto de Investigaciones Geológicas, Santiago, Carta Geológica de Chile, 1:50.000, 11.

Flint, S., Turner, P., Jolley, E.J., Hartley, A.J., 1993. Extensional tectonics in convergent margin basins: an example from the Salar de Atacama. *Chil. Andes. Geol. Soc. Am. Bull.* 105, 603-617.

Gardeweg, M., Ramírez, C.F., Davidson, J., 1993. Mapa Geológico del área Salar de Punta Negra y Volcán Lullaillaco, Región de Antofagasta. *Serv. Nac. Geol. Min. Doc. Trab.* 5 (1:100.000).

Gardeweg, M., Pino, H., Ramírez, C.F., Davidson, J., 1994. Mapa Geológico del área de Imilac y Sierra Almeida, Región de Antofagasta. *Serv. Nac. Geol. Min. Doc. Trab.* 7 (1:100.000).

Giambiagi, L., Ramos, V., Godoy, E., Alvarez, P., Orts, D., 2003. Cenozoic deformation and tectonic style of the Andes, between 33 and 34 south latitude. *Tectonics*. <http://dx.doi.org/10.1029/2001TC001354>.

González, R., Wilke, G.H., Menzies, A.H., Riquelme, R., Herrera, C., Matthews, S., Espinoza, F., Cornejo, P., 2015. Carta Sierra de Varas, Región de Antofagasta. Servicio Nacional de Geología y Minería, Carta Geológica de Chile. Serie Geología Básica 178, 1 mapa escala 1:100.000.

Hammerschmidt, K., Döbel, R., Friedrichsen, H. 1992. Implication of $^{40}\text{Ar}/^{39}\text{Ar}$ dating of Tertiary volcanics rocks from the north-Chilean Precordillera. *Tectonophysics*, 202, 55–81.

Hartley, A., Flint, S., Turner, P. & Jolley, E. J. 1992. Tectonic controls on the

development of a semi-arid alluvial basin as reflected in the stratigraphy of the Purilactis Group (Upper Cretaceous-Eocene) northern Chile. *Journal of South American Earth Sciences*, 5, 275–296.

Iaffa, D., S abat, F., Mu~noz, J.A., Mon, R., Gutierrez, A.A., 2011. The role of inherited structures in a foreland basin evolution. The Metan Basin in NW Argentina. *J. Struct. Geol.* 33, 1816e1828.

Isacson, P., Fischer, L., Davidson, J. 1985. Devonian and Carboniferous stratigraphy of Sierra de Almeida, Northern Chile, preliminary results. *Revista Geológica de Chile*, 25/26, 113–124.

Jaillard, E., 1992. La Fase Peruana (Cretáceo Superior) en la Margen Peruana. *Bol. Soc. Geol. Perú*, 83, 81–87.

Jordan, T., Muñoz, N., Hein, M., Lowenstein, T., Godfrey, L., Yu, J., 2002. Active faulting and folding without topographic expression in an evaporitic basin, Chile. *Geol. Soc. Am. Bull.* 114 (11), 1406-1421.

Jordan, T.E., Mpodozis, C., Muñoz, N., Blanco, N., Pananont, P., Gardeweg, M. 2007. Cenozoic subsurface stratigraphy and structure of the Salar de Atacama basin, northern Chile. *Journal of South American Earth Sciences*, Vol. 23, p. 122-146.

Kley, J., Monaldi, C., Salfity, J.A., 1999. Along-strike segmentation of the Andean foreland: causes and consequences. *Tectonophysics* 301, 75-94.

Kley, J., Rossello, E.A., Monaldi, C.R., Habighorst, B., 2005. Seismic and field evidence for selective inversion of Cretaceous normal faults, Salta rift, northwest Argentina. *Tectonophysics* 399, 55-172.

Kuhn, D., 2002. Fold and thrust belt structures and strike-slip faulting at the SE margin of the Salar de Atacama basin, Chilean Andes. *Tectonics*. doi:10.1029/2001TC901042.

Maksaev, V., 1990. Metallogeny, Geological Evolution and Thermochronology of the Chilean Andes between Latitudes 21 and 26 South, and the Origin of the Major Porphyry Copper Deposits. Tesis doctoral. Dalhousie University, Halifax, p. 544.

Maksaev, V., Zentilli, M., 1999. Fission track thermochronology of the Domeyko Cordillera, northern Chile: implications for Andean tectonics and porphyry copper metallogenesis. *Explor. Min. Geol.* 8, 65-89.

Marinovic, N., Lahsen, A.1984. Hoja Calama. Región de Antofagasta. Servicio Nacional de Geología y Minería, Carta Geológica de Chile, No. 58: 150 p., 1 mapa escala 1:250.000.

Marinovic, N., Smoje, I., Maksaev, V., Hervé, M., Mpodozis, C., 1995. Hoja Aguas

Blancas, Región de Antofagasta. Serv. Nac. Geol. Min. Doc. Trab. 70.

Martínez, F., Arriagada, C., Peña, M., Del Real, I., Deckart, K., 2013. The structure of the Chañarcillo Basin: an example of tectonic inversion in the Atacama region, northern Chile. *J. S. Am. Earth Sci.* 42, 1-16.

Martínez, F., Arriagada, C., Peña, M., Deckart, K., Charrier, R., 2016. Tectonic styles and crustal shortening of the Central Andes "Pampean" flat-slab segment in northern Chile (27°-29°S). *Tectonophysics* 667, 144-162.

Martínez, F., González, R., Bascuñan, S., Arriagada, C. 2017. Structural styles of the Salar de Punta Negra Basin in the Preandean Depression (24°-25°S) of the Central Andes, *Journal of South American Earth Sciences*. <http://dx.doi.org/10.1016/j.jsames.2017.08.004>.

Mescua, J., Giambiagi, L., 2012. Fault inversion vs. new thrust generation: a case study in the Malargüe fold-and-thrust belt, Andes of Argentina. *J. Struct. Geol.* 31, 51e63.

Monaldi, C.R., Salfity, J.A. and Kley, J., 2008. Preserved extensional structures in an inverted Cretaceous rift basin, northwestern Argentina: Outcrop examples and implications for fault reactivation. *Tectonics*, 27. doi: 10.1029/2006TC001993.

Mora, A., T. Gaona, J. Kley, D. Montoya, M. Parra, L. I. Quiroz, G. Reyes, and M. R. Strecker. 2009. The role of inherited extensional fault segmentation and linkage in contractional orogenesis: A reconstruction of Lower Cretaceous inverted rift basins in the Eastern Cordillera of Colombia, *Basin Res.*, 21, 111 – 137.

Mora, A., Horton, B.K., Mesa, A., Rubiano, J., Ketcham, R.A., Parra, M., Blanco, V., Garcia, D., Stockli, D.F. 2010. Cenozoic deformation patterns in the Eastern Cordillera, Colombia: Inferences from fission track results and structural relationships. *Reporte Interno, UTexas-ICP*.

Mpodozis, C., Cornejo, P., 1997. El rift Triásico-Sinemuriano de Sierra Exploradora, Cordillera de Domeyko (25 e26S): asociaciones de facies y reconstrucción tectónica. VIII Congreso Geológico Chileno. Antofagasta, Actas I. Sesión Temática 3, 550-554.

Mpodozis, C. and Ramos, V. A. 1989. The Andes of Chile and Argentina. In: Ericksen, G. E., Cañas, M. T., Reinemund, J. A. (eds) *Geology of the Andes and its Relation to Hydrocarbon and Energy Resources*. Circum-Pacific Council for Energy and Hydrothermal Resources, American Association of Petroleum Geologists, Houston, Texas, *Earth Science Series*, 11, 59-90.

Mpodozis, C. and Ramos, V. 2008. Tectónica Jurásica en Argentina y Chile: extensión, subducción oblicua, rifting, deriva y colisiones?, *Revista de la Asociación geológica Argentina*, 63, 479-495, 2008.

Mpodozis, C., Marinovic, N., Smoje, I., and Cuitiño, L., 1993. Estudio geológico-estructural de la Cordillera de Domeyko entre Cerro Limón Verde y Sierra Mariposas, Región de Antofagasta: Servicio Nacional de Geología y Minería [Chile], Santiago, Informe Registrado IR-93-04, 282 p.

Mpodozis, C., Arriagada, C. & Roperch, P. 1999. Cretaceous to Paleogene Geology of the Salar de Atacama Basin, Northern Chile: A reappraisal of the Purilactis Group Stratigraphy. Proceedings 4th International Symposium on Andean Geodynamics (ISAG), Göttingen, Germany, 523–526.

Mpodozis, C., Blanco, N., Jordan, T., Gardeweg, M.C., 2000. Estratigrafía y deformación del Cenozoico tardío en la región norte de la Cuenca del Salar de Atacama: La zona de Vilama-Pampa Vizcachitas. In: Actas IX Congreso Geológico Chileno, Puerto Varas, vol. 2, pp. 598-603.

Mpodozis, C., Arriagada, C., Basso, M., Roperch, P., Cobbold, P., Reich, M., 2005. Late Mesozoic to Paleogene stratigraphy of the Salar Atacama Basin, Antofagasta, Northern Chile: implications for the tectonic evolution of the central Andes. Tectonophysics 399, 125-154.

Muñoz, N., Charrier, R., Reutter, J. K. 1997. Evolución de la Cuenca del Salar de Atacama: Inversión tectónica y relleno de una cuenca de antepaís de retroarco. Proceedings 8th Congreso Geológico Chileno, 1, 195–199.

Muñoz, N., Charrier, R., Jordan, T., 2002. Interactions between basement and cover during the evolution of the Salar de Atacama Basin, Northern Chile. Rev. Geol. Chile 29, 55-80.

Niemeyer, H. 1984. La megafalla Tucúcaro en el extremo sur del Salar de Atacama: Una Antigua zona de cizalle reactivada en el Cenozoico. Departamento de Geología, Universidad de Chile, Santiago, Comunicaciones, 34, 37–45.

Niemeyer, H. 1989. El Complejo Igneo-Sedimentario del Cordón de Lila, Región de Antofagasta: significado tectónico. Revista Geológica de Chile, 16(2), 163–181.

Niemeyer, H., Urzua, F., Rubinstein, C., 1997. Nuevos antecedentes estratigraficos y sedimentologicos de la Formacion Zorritas, Devonico-Carbonifero de Sierra Almeida. Reg. Antofagasta, Chile Rev. Geol. Chile 24 (1), 25-43.

Padilla, H., 1985. Informes de avance, Enero y Febrero, proyecto “Geología regional de enlace entre Quebrada de Vaquillas y Salar de Pedernales”. Archivo técnico ENAP-Magallanes.

Pananont, P., C. Mpodozis, N. Blanco, T. E. Jordan, and L. D. Brown. 2004. Cenozoic evolution of the northwestern Salar de Atacama Basin, northern Chile, Tectonics, 23,

TC6007, doi:10.1029/2003TC001595.

Ramirez, C.; Gardeweg, P., 1982. Hoja Tocona, Región de Antofagasta. Servicio Nacional de Geología y Minería, Carta Geológica de Chile, 58: mapa escala 1:250.000, p. 1-121, Santiago.

Reutter, K.J., Charrier, R., Götze, H.J., Schurr, B., Wigger, P., Scheuber, E., Giese, P., Reuther, C.D., Schmidt, S., Rietbrock, A., Chong, G., Belmonte-Pool, A., 2006. The Salar de Atacama Basin: a subsiding block within the western edge of the Altiplano-Puna Plateau. In: Oncken, O., et al. (Eds.), *The Andes Active Subduction Orogeny*. Springer Berlin Heidelberg, Berlin, pp. 303-325.

Rubilar, J., Martínez, F., Arriagada, C., Becerra, J. 2017. Structure of the Cordillera de la Sal: A key tectonic element for the Oligocene-Neogene evolution of the Salar de Atacama basin, Central Andes, northern Chile, *Journal of South American Earth Sciences.*, <https://doi.org/10.1016/j.jsames.2017.11.013>

Rubinstein, C.V., Petus, E., Niemeyer, H. 2016. Palynostratigraphy of the Zorritas Formation, Antofagasta region, Chile: Insights on the Devonian/Carboniferous boundary in western Gondwana, *Geoscience Frontiers*, doi: 10.1016/j.gsf.2016.04.005.

Scheuber, E. and González, G. 1999. Tectonics of the Jurassic – Early Cretaceous magmatic arc of the north Chilean Coastal Cordillera (22°–26°S): A story of crustal deformation along a convergent plate boundary. *Tectonics*, 18, 895–910.

Scisciani, V., Tavarnelli, E., Calamita, F., 2002. The interaction of extensional and contractional deformations in the outer zones of the Central Apennines, Italy. *Journal of Structural Geology* 24, 1647–1658.

Scisciani, V. 2009. Styles of positive inversion tectonics in the Central Apennines and in the Adriatic foreland: Implications for the evolution of the Apennine chain (Italy), *Struct. Geol.* doi:10.1016/j.jsg.2009.02.004

Soto R., Martinod J., Riquelme R., Hérail G., Audin L., 2005. Using geomorphological markers to discriminate Neogene tectonic activity of North Chilean forearc (24°-25° S), *Tectonophysics* 41, p. 41-55.

Tomlinson, A., Blanco, N. 1997. Structural evolution and displacement history of the West fault System, Precordillera, Chile: Part 1 y 2, synmineral history. In: *Proceedings 8th Congreso Geológico Chileno, Antofagasta, 3, 1873–1882.*

Figure captions

Fig. 1. Location of the Preandean Depression in the Central Andes, northern Chile, and distribution of neighboring tectonic provinces in Chile, Argentina, and Bolivia.

Fig. 2. Simplified geological map showing the plan-view distribution of major tectonic provinces and geological units that form part of the forearc of northern Chile, between 23° and 24°30' S.

Fig. 3. Simplified geological map over a Landsat 8 image of the Salar de Atacama Basin (modified from Arriagada et al., 2006 and Bercerra et al., 2014) and location of the 2-D seismic profiles used in this study (red lines). K-Ar and U-Pb ages were taken from Mpodozis et al. (2005) and Bascuñan et al. (2015). The yellow stars indicate the location of photographs in Figs 5 and 6. The white dotted lines indicate stratification. Abbreviations: Paleozoic-Triassic rocks: Lila Complex; Cretaceous: Purilactis Group; Paleocene intrusives: Paleocene granitic rocks; Paleocene-Eocene successions: Naranja Formation; Oligocene-Miocene successions: San Pedro and Tambores (Paciencia Group) fms; Miocene ignimbrites; Quaternary volcanic deposits: mainly lavas and ignimbrites. Location of the Toconao-1 oil well is indicated.

Fig. 4. Simplified geological map over a Landsat 8 image of the Salar de Punta Negra Basin and the eastern part of the Domeyko Cordillera (modified from Gardeweg et al., 1993, 1994 and González et al., 2015) and location of the 2-D seismic profiles used in this study (red lines). The yellow star indicates the location of the photographs in Fig. 7. The white and black dotted lines indicate stratification. Abbreviations: Paleozoic-Triassic rocks: Zorritas and/or La Tabla fms; Triassic: Sierra de Varas Formation; Jurassic: El Profeta Formation; Oligocene-Miocene successions: Pampa de Mulas Formation; Miocene ignimbrites.

Fig. 5. a) View of the contact relationship between the Tonel and Purilactis formations of the Purilactis Group, b) meso-scale reverse faulting and folding affecting the Oligocene-Miocene deposits of the Paciencia Group (San Pedro Formation), and c) view of the folded unconformity between the Paciencia Group and the deformed Miocene ignimbrites exposed along the Salar de Atacama Basin. See Fig. 3 for location.

Fig. 6. a) W-E view of the growth strata preserved within synorogenic deposits of the Purilactis Group, b) detail of the angular unconformity between the synorogenic deposits of the upper Purilactis Group and the Miocene ignimbrites exposed along the Barros Arana

Syncline, and c) plan-view aspect of the Paciencia Fault bounding the western flank of the Cordillera de la Sal from the Llano de la Paciencia region. See Fig. 3 for location.

Fig. 7. a) Detail of the folded and faulted angular unconformity between the Oligocene-Miocene synorogenic deposits of the San Pedro Formation and the Miocene ignimbrites along the northern part of the Salar de Atacama Basin, and b) panoramic view showing traces of the basement-involved reverse faults that affect the western edge of the Salar de Punta Negra Basin. See Figs. 3 and 7 for location.

Fig. 8. Stratigraphic template showing the proposed correlation between the tectonosequences interpreted in this work and the geological units exposed along the Salar de Atacama and Salar de Punta Negra basins. The seismic profile corresponds to the central section of line IG010 located along the central part of the Salar de Atacama Basin. The projection of the Toconao-1 oil well is indicated into the seismic data. Abbreviations: SAB: Salar de Atacama Basin, SPNB: Salar de Punta Negra Basin.

Fig. 9. Cartoon illustrating the main extensional and contractional interaction styles recognized in the Preandean basins.

Fig. 10. Uninterpreted and interpreted 2-D seismic profile IG08b, showing a pair of partially inverted half-graben structures along the central section of the Salar de Atacama Basin. See Fig. 3 for location. T1-T2: Upper Paleozoic-Jurassic syn-rift tectonosequences; T3: Upper Cretaceous-Paleocene synorogenic tectonosequences; T4: Eocene synorogenic tectonosequences; T5: Oligocene-Miocene synorogenic tectonosequences; T6: Mio-Pliocene synorogenic tectonosequences.

Fig. 11. Uninterpreted and interpreted 2-D seismic profile IG016b, showing the structural interaction between extensional and contractional structures along the south-central section of the Salar de Atacama Basin. The seismic profile shows a good example of decapitation of normal faults by reverse faults. See Fig. 3 for location. T1 to T6 presented as in Fig. 10.

Fig. 12. Uninterpreted and interpreted eastern segment of the 2-D seismic profile IG024. The seismic interpretation shows two types of structural interaction: normal faults by reverse faults and the transport of normal faults by a thrust ramp. See Fig. 3 for location. T1 to T6 presented as in Fig. 10.

Fig. 13. Uninterpreted and interpreted western segment of the 2-D seismic profile IG024, showing the main structural styles (inversion anticline and basement-involved reverse faults) observed along the south and easternmost part of the Salar de Atacama Basin. See Fig. 3 for location. T1 to T6 presented as in Fig. 10.

Fig. 14. Uninterpreted and interpreted 2-D seismic profile 1F016, showing decapitation of the upper section of a partially inverted normal fault by basement-involved faults in the northern part of the Salar de Punta Negra Basin (Modified from Martínez et al., 2017). See Fig. 4 for location. T1 to T6 presented as in Fig. 10.

Fig. 15. Uninterpreted and interpreted 2-D seismic profile 2F004, showing a series of doubly-dipping inverted faults and folds, which reveal the positive tectonic inversion of previous normal faults in the north-central part of the Salar de Punta Negra Basin (Modified from Martínez et al., 2017). See Fig. 4 for location. T1 to T6 presented as in Fig. 10.

Highlights

- We analyse extensional and contractional structures in the Preandean Depression
- We use 2-D seismic profiles of these basins, supported by field data
- We reveal three interaction types between extensional and contractional structures
- Synorogenic tectonosequences recorded the tectonic evolution of the region
- Basement-related reverse fault structures were responsible for crustal thickening

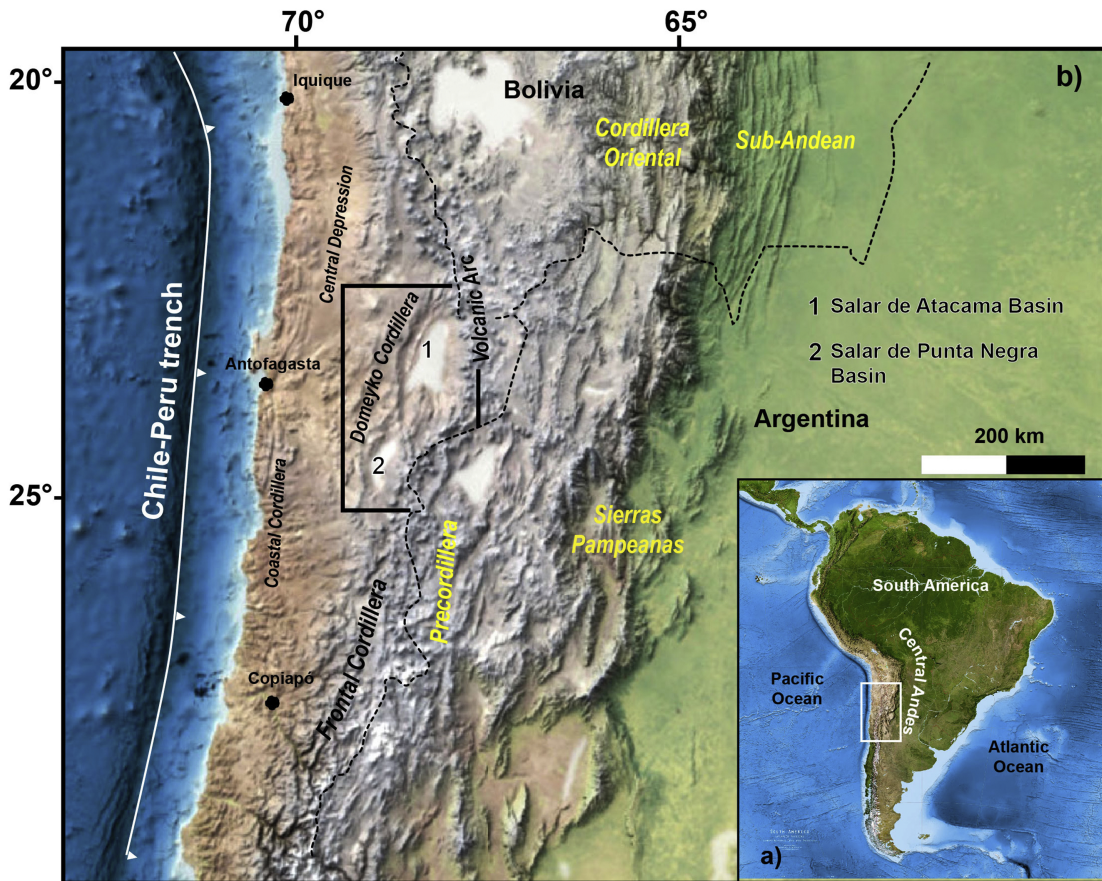

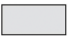










Figure 1

LEGEND

-  Salt flats
-  Pleistocene volcanics
-  Mio-Pliocene gravels deposits
-  Oligocene-Miocene deposits
-  Cretaceous-Paleocene deposits
-  Cretaceous-Paleocene intrusives
-  Paleozoic-Triassic basement

SYMBOLS

-  Major faults
-  El Bordo Escarpment
-  Syncline folds

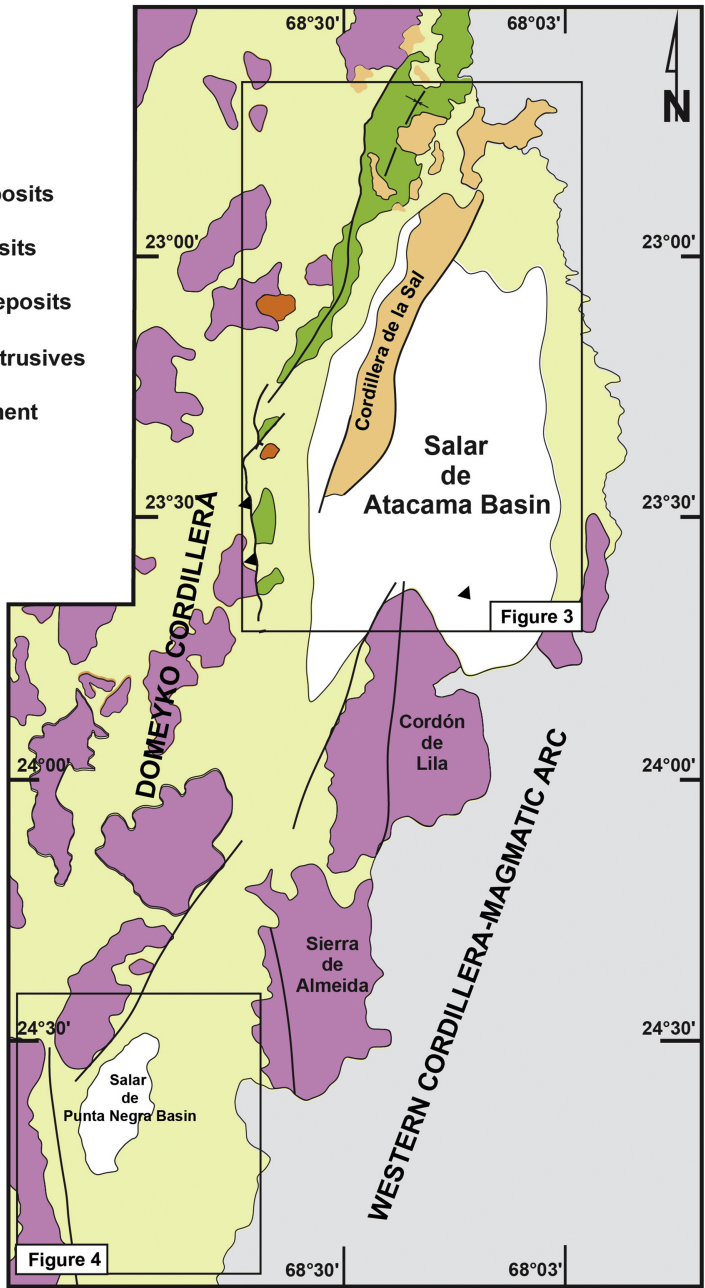


Figure 2

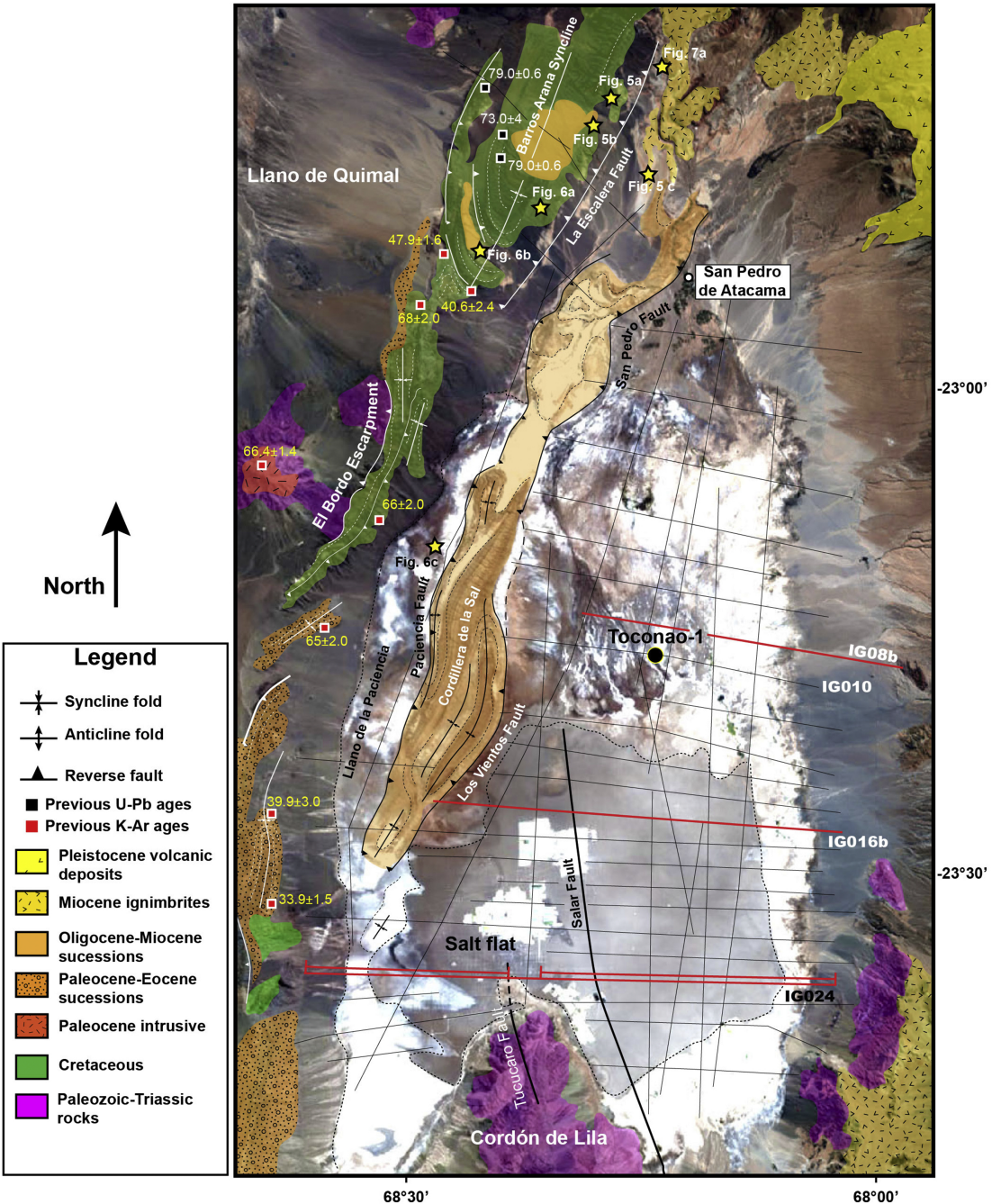


Figure 3

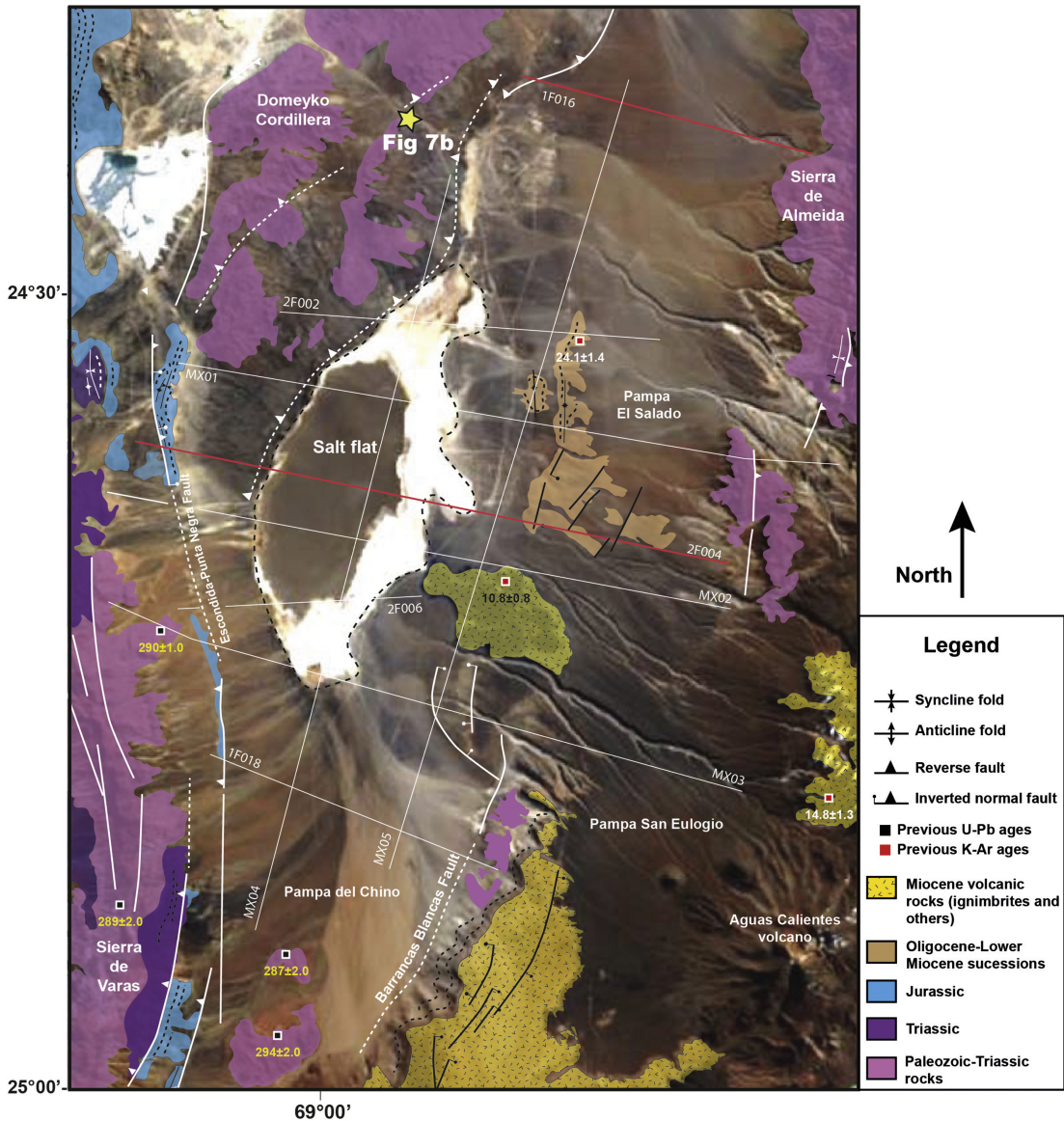


Figure 4

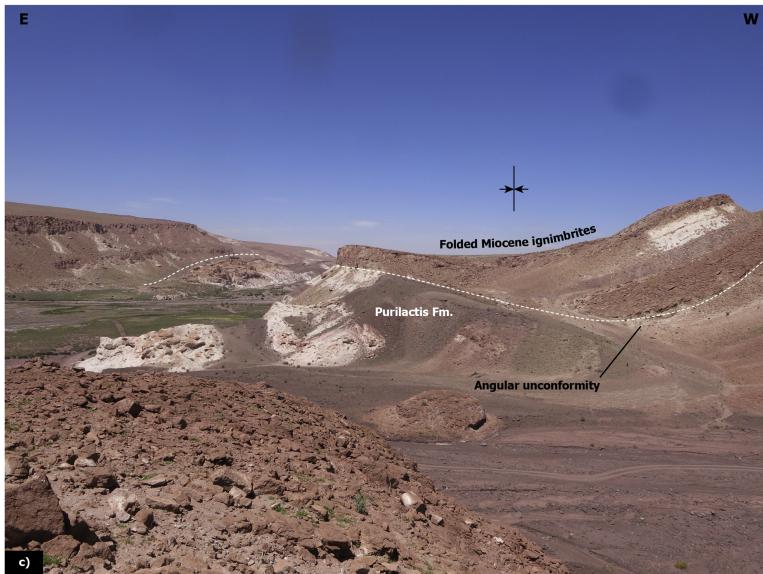
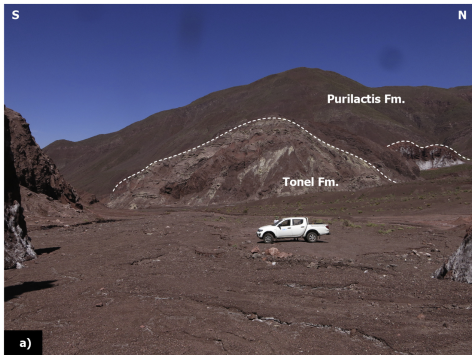


Figure 5

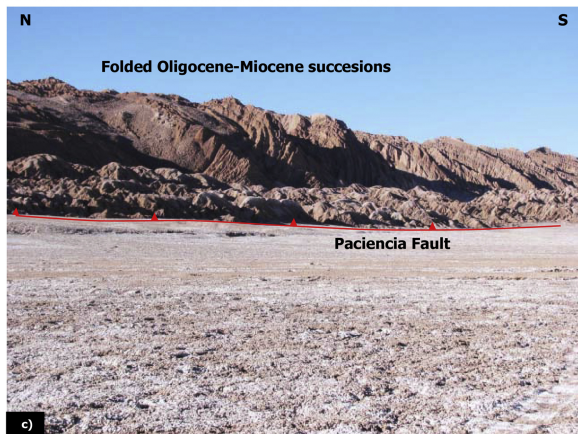


Figure 6

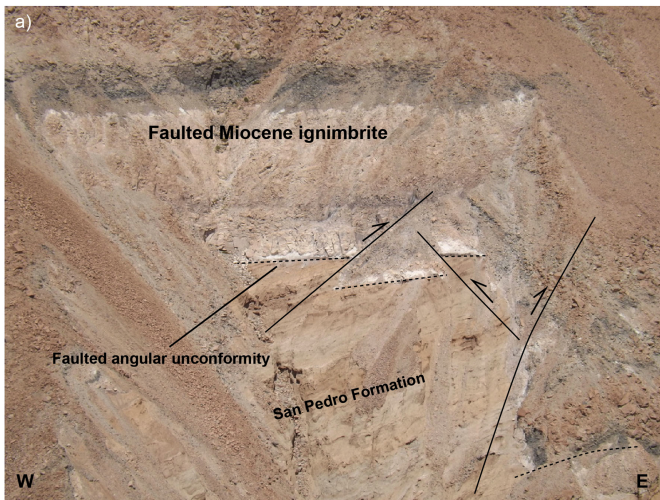


Figure 7

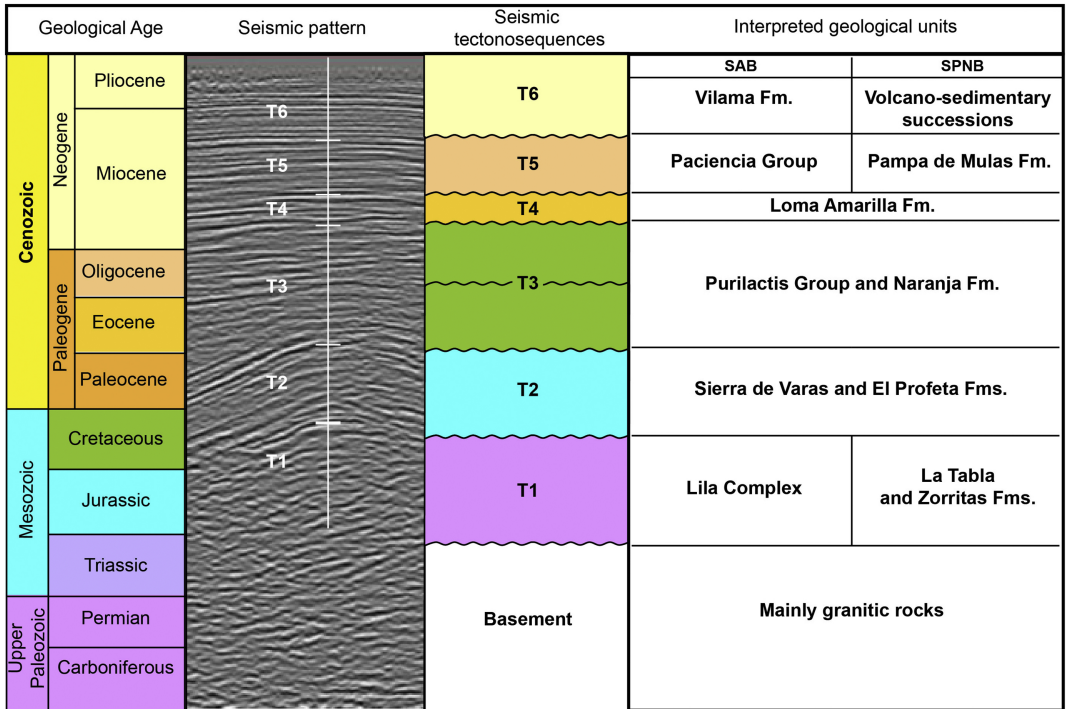
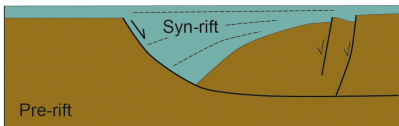


Figure 8

Initial pre-shortening state

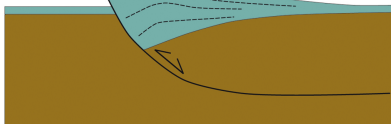
Extensional fault system



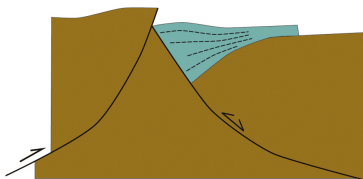
Rollover and synthetic and antithetic faults

Shortening and basin inversion

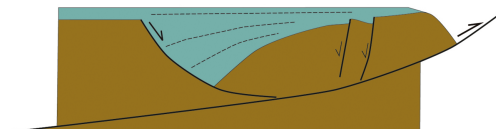
Pure positive inversion



Inversion anticline



Decapitation of previous inverted normal fault



Transport of previous inverted normal fault by thrust ramp

Figure 9

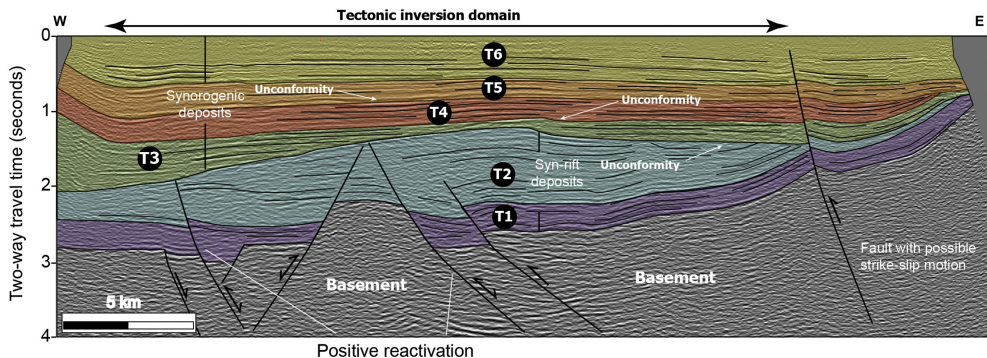
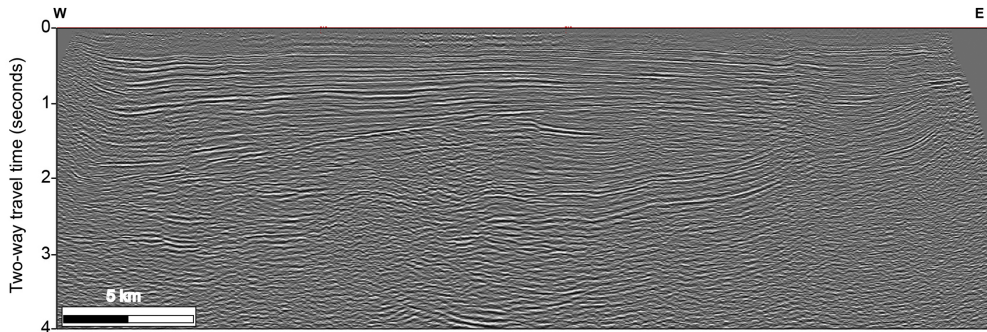
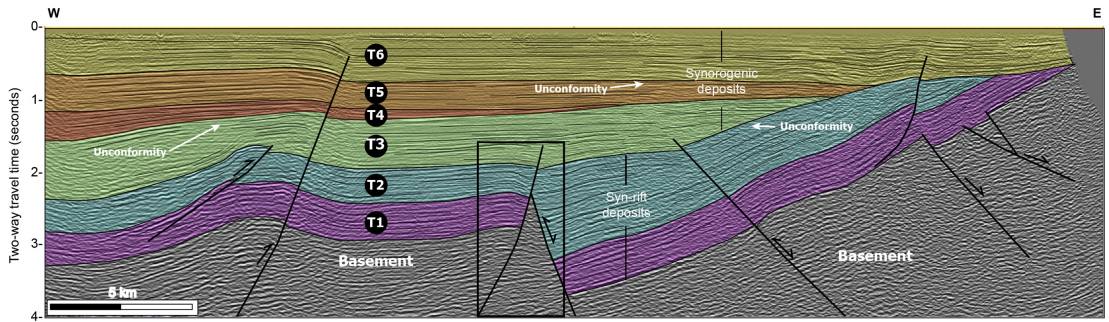
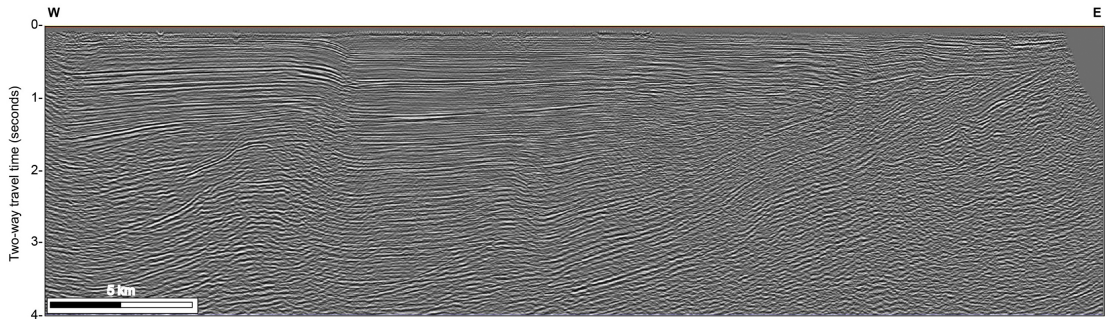
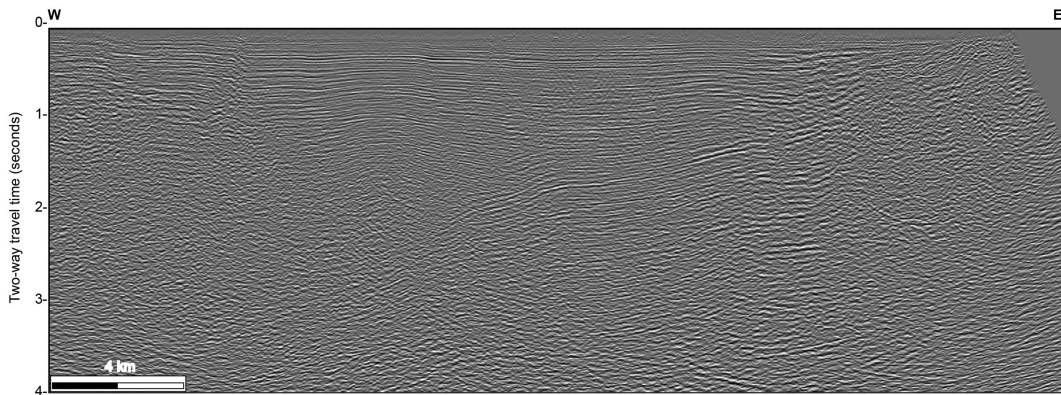


Figure 10



Decapitation of a previous inverted fault

Figure 11



Decapitation of a previous inverted fault

West-dipping
reverse faulting

Tectonic inversion domain

East-dipping reverse faulting

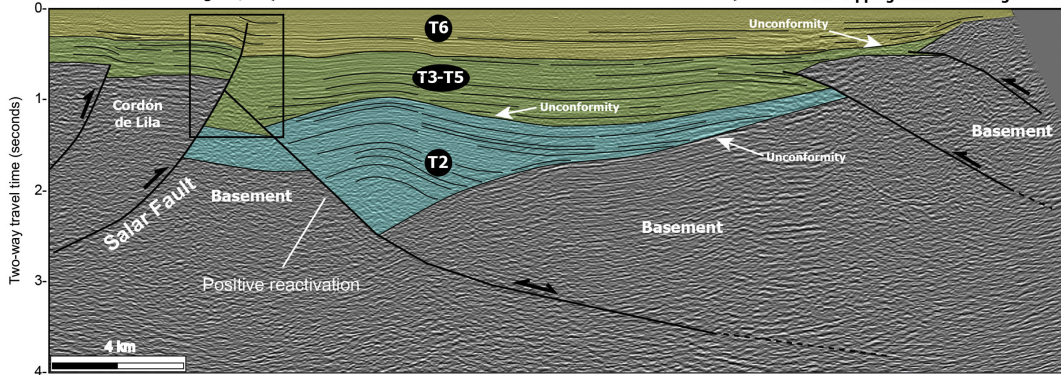


Figure 12

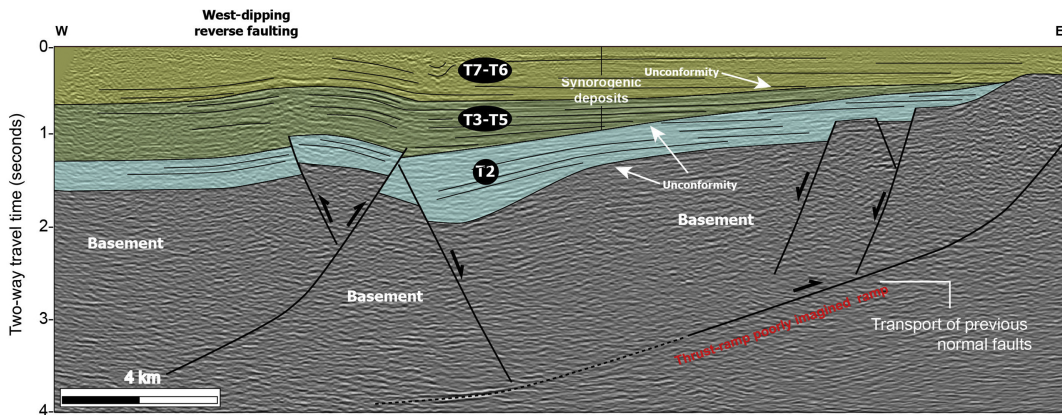
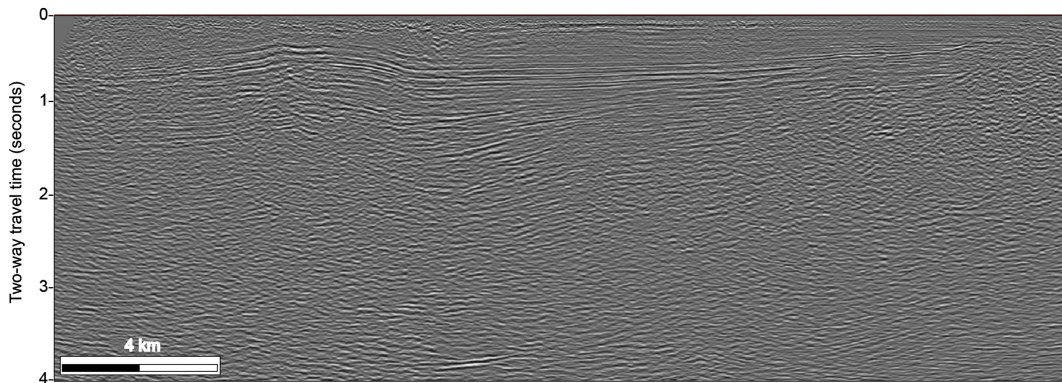


Figure 13

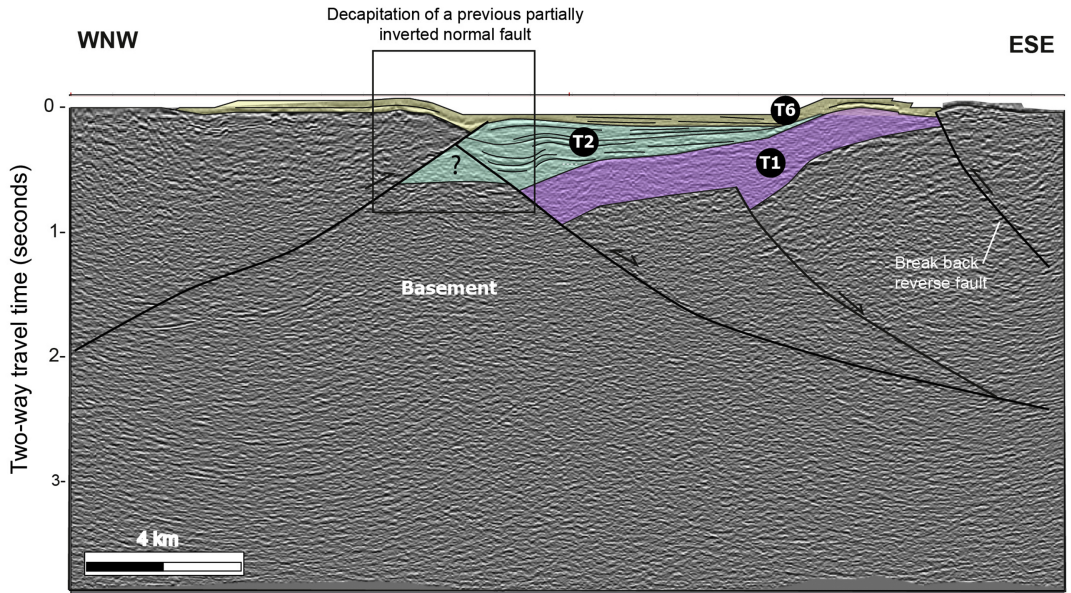
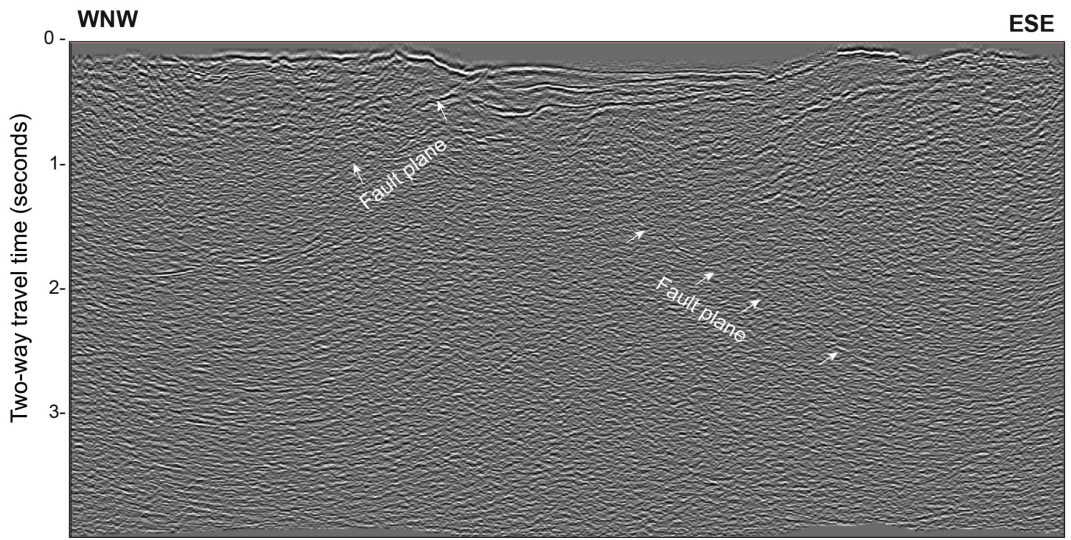


Figure 14

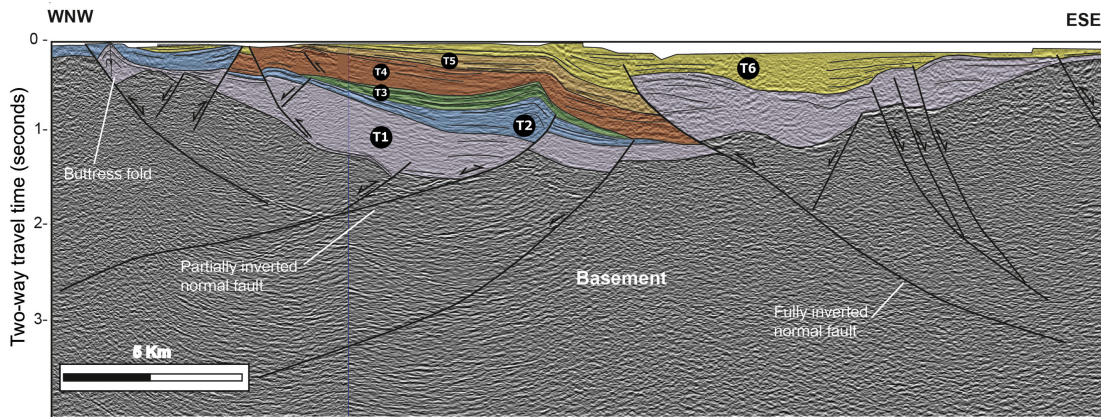
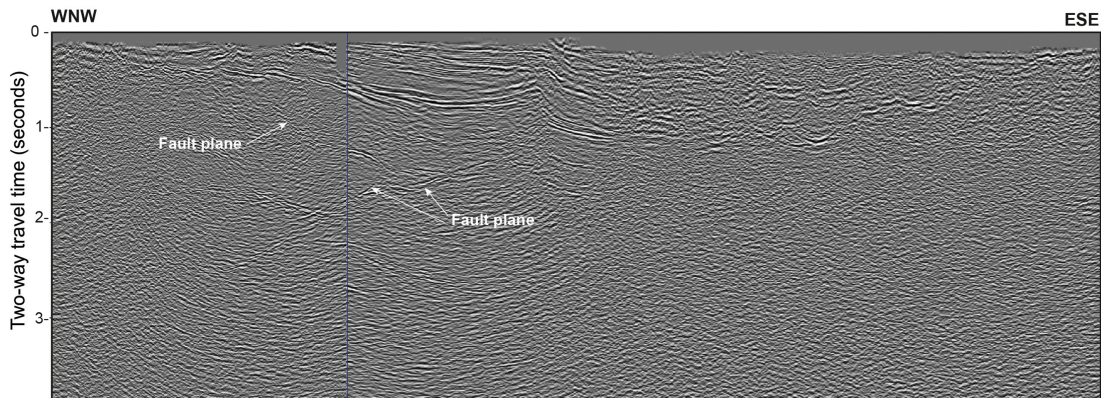


Figure 15